Chapter 9
Holography for Inflationary Cosmology

Paul McFadden

Abstract We review the construction of a holographic framework for cosmology enabling four-dimensional inflationary universes to be described in terms of three-dimensional dual quantum field theories. We show how cosmological observables are encoded in the correlation functions of the dual QFT, and obtain precise holographic formulae for the primordial power spectra. Through perturbative QFT calculations, we compute holographically the observational signatures of a universe emerging from a non-geometric phase in which the gravitational description is strongly coupled at early times. A custom fit to WMAP7 and other astrophysical data allows us to estimate the parameters of the holographic model and assess its performance relative to standard power-law ΛCDM.

9.1 Introduction

The notion of holography first emerged from considerations of black hole physics. In [49],'t Hooft observed that the onset of gravitational collapse imposes an upper bound on the entropy of any given region of spacetime. Through simple scaling arguments, he showed that the configuration with the maximum possible entropy consists of a single black hole completely filling the region, whose entropy then scales as the area of the region's boundary in Planck units. Since entropy is a measure of the number of (Boolean) degrees of freedom, it follows that the number of degrees of freedom in any gravitational theory scales as the area of the boundary. In particular, the gravitational entropy scales in the same way as the ordinary extensive entropy of a non-gravitational QFT living in one dimension less. Driving this argument to its ultimate conclusion [47, 49], one arrives at the *holographic principle*: that any quantum gravitational system should admit an equivalent dual description in terms of a non-gravitational QFT living in one dimension less.

Astonishingly, a concrete realisation of this conjecture—the AdS/CFT correspondence—was subsequently found in string theory [30], and a precise holographic

P. McFadden (✉)
Perimeter Institute for Theoretical Physics, Waterloo, ON, Canada N2J 2Y5
e-mail: pmcfadden@perimeterinstitute.ca

G. Calcagni et al. (eds.), *Quantum Gravity and Quantum Cosmology*,
Lecture Notes in Physics 863, DOI 10.1007/978-3-642-33036-0_9,

dictionary linking bulk and boundary quantities was established soon thereafter [16, 53]. In spite of the generality of 't Hooft's original argument, however, almost all explicit realisations of holography to date necessarily involve spacetimes with a negative cosmological constant. The extent to which holographic dualities may be extended to encompass more general spacetimes is an unanswered question of the greatest importance.

One promising strategy is to start with spacetimes closely related to those already in possession of a well understood holographic description. Inflationary cosmologies provide just such an example, and of course are of great interest in their own right. In a recent series of papers [7, 14, 33–37] we proposed how to set up a holographic framework for cosmology, enabling cosmological evolution to be described through the physics of a dual three-dimensional non-gravitational QFT. While our chief focus is the primordial inflationary epoch, the framework we propose may also be applied to the late-time de Sitter epoch our universe is currently entering. In this article, we will review this basic holographic framework and discuss the holographic calculation of the cosmological power spectrum, expanding and updating our earlier account[1] [35].

Aside from the conceptual interest attached to a holographic description of inflationary cosmology, there are a number of more pragmatic reasons motivating such a development. Firstly, uncovering the structure of three-dimensional QFT in cosmological observables brings in new intuition about their structure and may lead to more efficient computational techniques, particularly for the calculation of non-Gaussianities. Secondly, the standard inflationary scenario, despite its successes, is still unsatisfactory in a number of ways: it generically requires fine tuning, and there are trans-Planckian issues and questions about the initial conditions for inflation, see for instance [6, 50]. A key feature of known holographic dualities is their strong/weak coupling nature, meaning that in the regime where the one description is weakly coupled the other is strongly coupled. A holographic framework for cosmology thus provides a natural arena for constructing new models with intrinsic strong-coupling gravitational dynamics at early times—a holographic non-geometric phase—that have only a weakly coupled three-dimensional QFT description. Such models lie beyond the scope of the conventional inflationary paradigm, and may potentially be free from the problems besetting conventional inflationary models. Moreover, as we will see, models of this nature generically lead to qualitatively different predictions for cosmological observables that will be measured in the near future.

Any holographic proposal for cosmology should specify what the dual QFT is and how to use it to compute cosmological observables. The holographic description we propose uses the one-to-one correspondence between cosmologies and so-called 'domain-wall' spacetimes discussed in [9, 45], and assumes that standard holographic dualities (also known as gauge/gravity dualities, since the dual QFT

[1] The slides for the talk accompanying these proceedings may also be found online at http://www.physics.ntua.gr/cosmo11/Naxos2011/MorningLectures/McFadden.pdf.

is typically a large-N gauge theory) are valid. More precisely, the steps involved are illustrated in Fig. 9.1. The first step is to map any given inflationary spacetime to a domain-wall spacetime. For cosmologies that at late times approach either a de Sitter spacetime or a power-law scaling solution, the corresponding domain-wall solutions describe holographic renormalisation group flows (i.e., spacetimes in which the radial evolution of the bulk geometry holographically encodes RG flow in the dual QFT). For these cases there is an operational gauge/gravity duality, meaning one has a dual description in terms of a three-dimensional QFT. Crucially, the map between cosmologies and domain-walls may equivalently be expressed entirely in terms of QFT variables, and amounts to a certain analytic continuation of parameters and momenta. Applying this analytic continuation to the regular QFT dual to the domain-wall spacetime, we obtain the QFT dual of the original cosmological spacetime.

We call this latter theory a 'pseudo'-QFT because we currently only have an operational definition for it, namely, we do the computations in the regular QFT dual to the corresponding domain-wall spacetime and then apply the analytic continuation. From the standard holographic dictionary, to compute tree-level cosmological correlators we need continue only the large-N correlators of the dual QFT, where N is the rank of the gauge group of the dual QFT. (Loop corrections to cosmological correlators then correspond to $1/N^2$ corrections in the dual QFT.) In the large-N limit, this analytic continuation is well defined and simply amounts to the insertion of a few minus signs in specific formulae. Thus, from a strictly pragmatic point of view, our operational definition of the pseudo-QFT is sufficient to compute all observable quantities of interest. Nonetheless, one might ultimately hope for a more fundamental definition, in particular one that is valid beyond large-N perturbation theory. Interesting progress along these lines (albeit for a very different bulk gravitational theory) was recently made in [1], where the pseudo-QFT dual to Vasiliev higher spin gravity on de Sitter space was identified as a specific $Sp(N)$ gauge theory.

The remainder of this article is organised as follows. In Sect. 9.2, we discuss the general features of domain-walls and cosmologies: the form of the background metric and perturbations, their dynamics, the domain-wall/cosmology correspondence, and the primordial cosmological power spectrum. In Sect. 9.3, we discuss holography for cosmology: the background solutions of interest, the basics of holography including the radial Hamiltonian formulation, properties of the stress tensor 2-point function, and the analysis required to derive holographic formulae for the cosmological power spectra. In Sect. 9.4, we introduce holographic phenomenology for cosmology, and discuss the computation of the holographic power spectra up to 2-loop order in perturbation theory. Finally, in Sect. 9.5, we discuss the observational compatibility of the predicted holographic power spectrum in the light of WMAP7 and other astrophysical data.

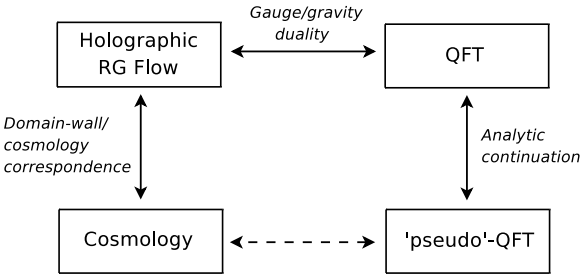

Fig. 9.1 The 'pseudo'-QFT dual to inflationary cosmology is operationally defined using the correspondence of cosmologies to domain-walls and standard gauge/gravity duality

9.2 Domain-Walls and Cosmologies

Let us begin by introducing the various objects appearing on the l.h.s. of Fig. 9.1, which represents the bulk gravitational physics. For simplicity, we will focus throughout on spatially flat universes with a single inflaton field, Φ, which we take to be minimally coupled and equipped with a potential $V(\Phi)$. All our results may straightforwardly be extended to more general cases if desired, (e.g., non-flat, multi-scalar, non-canonical kinetic terms, etc.).

9.2.1 Defining the Perturbations

The metric and scalar field for the unperturbed background solution take the form

$$\mathrm{d}s^2 = \sigma \mathrm{d}z^2 + a^2(z)\mathrm{d}x_i\mathrm{d}x^i, \qquad \Phi = \varphi(z), \tag{9.1}$$

where the spatial index i runs from 1 to 3, and σ is a sign taking values $\sigma = \pm 1$. If $\sigma = -1$, the metric describes a flat FRW cosmology with z the proper time co-ordinate. The remaining case, where $\sigma = +1$, we will refer to as a domain-wall spacetime.[2] In this latter case, z now plays the role of a radial coordinate. Note also that we have chosen the domain-wall to be Euclidean. A Lorentzian domain-wall may easily be obtained by continuing one of the x^i coordinates to become a time coordinate [45]. The continuation to a Euclidean domain-wall will turn out to be convenient, however, since the QFT vacuum state implicit in the Euclidean formulation maps to the Bunch-Davies vacuum on the cosmology side. (Other choices of cosmological vacuum require considering the boundary QFT in different states, which may be accomplished using the real-time formalism of [46].)

[2]The name 'domain-wall' spacetime dates back to earlier work featuring solutions of this form that interpolate between two stationary points of the scalar field potential, one at $z = +\infty$ and another at $z = -\infty$. Unfortunately in the present context the name is slightly misleading, since we consider only the $z > 0$ part of the geometry, i.e., there is no actual domain wall. We will nevertheless stick with this terminology as it is standard issue in high-energy physics.

Turning now to include perturbations, the inflaton may be decomposed into a background piece φ and a perturbation $\delta\varphi$,

$$\Phi(z,\mathbf{x}) = \varphi(z) + \delta\varphi(z,\mathbf{x}),$$

while the perturbed metric may be written in the ADM form

$$\mathrm{d}s^2 = \sigma N^2 \mathrm{d}z^2 + g_{ij}\big(\mathrm{d}x^i + N^i\mathrm{d}z\big)\big(\mathrm{d}x^j + N^j\mathrm{d}z\big), \tag{9.2}$$

where the perturbed lapse and shift functions

$$N = 1 + \delta N(z,\mathbf{x}), \qquad N_i = g_{ij}N^j = \delta N_i(z,\mathbf{x}), \qquad g_{ij} = a^2(z)\big(\delta_{ij} + h_{ij}(z,\mathbf{x})\big).$$

We may then further decompose the perturbations into scalar, vector and tensor pieces according to

$$\delta N_i = a^2(v_{,i} + v_i), \qquad h_{ij} = -2\psi\delta_{ij} + 2\chi_{,ij} + 2\omega_{(i,j)} + \gamma_{ij}, \tag{9.3}$$

where the vector perturbations v_i and ω_i are transverse, $v_{i,i} = 0$ and $\omega_{i,i} = 0$, while the tensor perturbation γ_{ij} is transverse traceless, $\gamma_{ij,i} = 0$ and $\gamma_{ii} = 0$. (Here, and in the remainder of this article, we adopt the convention that repeated covariant indices are summed using the Kronecker delta. In contrast, an index is raised or lowered using the full metric.)

Gauge-invariant variables may be defined by relating the perturbations in a general gauge to those in some fully-fixed gauge. We will see shortly that the dynamics comprise only a single scalar degree of freedom, plus one tensor mode. To parametrise this scalar degree of freedom, a particularly useful choice is the gauge-invariant variable $\zeta(z,\mathbf{x})$ encoding the curvature perturbation on uniform energy density slices. More precisely, ζ is defined so that in comoving gauge, where $\delta\varphi$ vanishes, the spatial part of the perturbed metric reads

$$g_{ij} = a^2 e^{2\zeta}\big[e^{\hat{\gamma}}\big]_{ij},$$

where $\hat{\gamma}_{ij}$ is transverse traceless and the exponential is to be expanded out (i.e., $[e^{\hat{\gamma}}]_{ij} = \delta_{ij} + \hat{\gamma}_{ij} + \cdots$). This prescription fixes the gauge completely, thereby defining the gauge-invariant variables ζ and $\hat{\gamma}_{ij}$ to all orders in perturbation theory. In our forthcoming discussion of the holographic power spectrum, however, we will only need to work to linear order in perturbation theory. In this case, upon transforming to a general gauge, we find ζ and $\hat{\gamma}_{ij}$ correspond to the gauge-invariant combinations

$$\zeta = -\psi - \frac{H}{\dot{\varphi}}\delta\varphi, \qquad \hat{\gamma}_{ij} = \gamma_{ij}.$$

The corresponding expressions at quadratic order in perturbation theory, as required for the treatment of non-Gaussianities, may be found in [36, 37]. (Note in particular that γ_{ij} is no longer gauge-invariant at quadratic order.)

Finally, when working in momentum space, it is useful to decompose the transverse traceless tensors in a helicity basis according to

$$\hat{\gamma}_{ij}(z,\mathbf{q}) = \sum_{s=\pm} \hat{\gamma}^{(s)}(z,\mathbf{q})\varepsilon_{ij}^{(s)}(\mathbf{q}), \tag{9.4}$$

where $\mathbf{q}$ is the spatial 3-momentum and the helicity tensors $\varepsilon_{ij}^{(s)}(\mathbf{q})$ are normalised so that

$$\varepsilon_{ij}^{(s)}(\mathbf{q})\varepsilon_{ij}^{(s')}(-\mathbf{q}) = 2\delta^{ss'}, \qquad \sum_{s=\pm} \varepsilon_{ij}^{(s)}(\mathbf{q})\varepsilon_{kl}^{(s)}(-\mathbf{q}) = 2\Pi_{ijkl}, \tag{9.5}$$

with the transverse traceless projector Π_{ijkl} and the transverse projector π_{ij} defined by

$$\Pi_{ijkl} = \frac{1}{2}(\pi_{ik}\pi_{jl} + \pi_{il}\pi_{jk} - \pi_{ij}\pi_{kl}), \qquad \pi_{ij} = \delta_{ij} - \frac{q_i q_j}{q^2}.$$

Note that with these normalisation conventions, $\hat{\gamma}^{(s)}(z,\mathbf{q}) = (1/2)\varepsilon_{ij}^{(s)}(-\mathbf{q})\hat{\gamma}_{ij}(z,\mathbf{q})$. Explicit expressions for the helicity tensors may be found in [37, 51]. Under complex conjugation, $\varepsilon_{ij}^{(s)*}(\mathbf{q}) = \varepsilon_{ij}^{(s)}(-\mathbf{q}) = \varepsilon_{ij}^{(-s)}(\mathbf{q})$.

9.2.2 Dynamics

Having written the metric in the ADM form (9.2), we may now write the action for both domain-walls and cosmologies in the combined form

$$\begin{aligned} S = \frac{1}{2\kappa^2}\int \mathrm{d}^4x N\sqrt{g}\big[&K_{ij}K^{ij} - K^2 + N^{-2}\big(\dot{\Phi} - N^i\Phi_{,i}\big)^2 \\ &+ \sigma\big(-R + g^{ij}\Phi_{,i}\Phi_{,j} + 2\kappa^2 V(\Phi)\big)\big]. \end{aligned} \tag{9.6}$$

Here, $\kappa^2 = 8\pi G$, R is the scalar curvature of the spatial metric g_{ij} and $K_{ij} = [(1/2)\dot{g}_{ij} - \nabla_{(i}N_{j)}]/N$ is the extrinsic curvature of constant-z slices. While this expression might seem unfamiliar, it is simply the action of gravity minimally coupled to a scalar field with a potential $V(\Phi)$ in disguise. Setting $\sigma = -1$ for example, the action (9.6) is equivalent to the familiar inflationary action

$$S_C = \frac{1}{2\kappa^2}\int \mathrm{d}^4x\sqrt{g^{(4)}}\big[R^{(4)} - (\partial\Phi)^2 - 2\kappa^2 V(\Phi)\big].$$

Our reason for preferring the ADM form (9.6) is simply that it neatly encompasses both *Lorentzian* cosmologies and *Euclidean* domain-walls: the spatial gradient and potential terms on the second line appear with positive sign for Euclidean domain-walls and with negative sign for Lorentzian cosmologies, while the kinetic terms on the first line take the same sign for both.

In the following, we will restrict our consideration to background solutions in which the evolution of the scalar field $\varphi(z)$ is (piece-wise) monotonic in z, as appropriate for describing holographic RG flows. For such solutions, $\varphi(z)$ can be inverted to $z(\varphi)$, allowing the Hubble rate $H \equiv \dot{a}/a$ to be expressed as a function of φ, say as $H(z) = -(1/2)W(\varphi)$. The complete equations of motion for the background then take the simple form

$$H = -\frac{1}{2}W, \qquad \dot{\varphi} = W_{,\varphi}, \qquad 2\sigma\kappa^2 V = (W_{,\varphi})^2 - \frac{3}{2}W^2. \tag{9.7}$$

In cosmology, this first-order formalism dates back to the work of [42], where it was obtained by application of the Hamilton-Jacobi method. For domain-walls, this formalism has been discussed from variety of standpoints in [10, 12, 15, 44, 45].

An action for the perturbations may be obtained by solving the Hamiltonian and momentum constraints for the comoving-gauge lapse and shift in terms of ζ and $\hat{\gamma}_{ij}$, then backsubstituting into (9.6). Keeping track of the sign σ, at quadratic order we find

$$S = \frac{1}{\kappa^2}\int \mathrm{d}^4x \left[a^3\varepsilon\dot{\zeta}^2 + \sigma a\varepsilon(\partial\zeta)^2 + \frac{a^3}{8}\dot{\hat{\gamma}}_{ij}\dot{\gamma}_{ij} + \frac{\sigma a}{8}\hat{\gamma}_{ij,k}\hat{\gamma}_{ij,k} \right], \tag{9.8}$$

where $\varepsilon = -\dot{H}/H^2 = \dot{\phi}^2/2H^2 = 2(W_{,\varphi}/W)^2$. (In standard inflation ε would be the usual slow-roll parameter, however we have no need to assume slow roll here.) The action at cubic order may be derived by the same method, albeit with more work; the result may be found in [31] (or including the sign σ, in [36]).

In momentum space, the corresponding linear equations of motion are

$$0 = \ddot{\zeta} + (3H + \dot{\varepsilon}/\varepsilon)\dot{\zeta} - \sigma a^{-2}q^2\zeta, \qquad 0 = \ddot{\hat{\gamma}}^{(s)} + 3H\dot{\hat{\gamma}}^{(s)} - \sigma a^{-2}q^2\hat{\gamma}^{(s)}. \tag{9.9}$$

From the first of these equations one finds that ζ tends to a constant on superhorizon scales for which $q \ll aH$. This property accounts for the utility of ζ in inflationary cosmology: perturbations exit the horizon during inflation, after which they remain constant until their eventual re-entry in the subsequent radiation- or matter-dominated eras.

Finally, in preparation for our holographic analysis to follow, it is useful to define *response functions* relating the canonical momenta to the perturbations. From the quadratic action (9.8), the canonical momenta (times an overall factor of κ^2) are

$$\Pi = \kappa^2\frac{\partial\mathscr{L}}{\partial\dot{\zeta}} = 2\varepsilon a^3\dot{\zeta}, \qquad \Pi_{ij} = \kappa^2\frac{\partial\mathscr{L}}{\partial\dot{\hat{\gamma}}_{ij}} = \frac{1}{4}a^3\dot{\hat{\gamma}}_{ij}. \tag{9.10}$$

In momentum space, we may further decompose Π_{ij} in a helicity basis,

$$\Pi_{ij}(z,\mathbf{q}) = \sum_{s=\pm}\Pi^{(s)}(z,\mathbf{q})\varepsilon_{ij}^{(s)}(\mathbf{q}), \qquad \Pi^{(s)}(z,\mathbf{q}) = \frac{1}{4}a^3\dot{\hat{\gamma}}^{(s)}(z,\mathbf{q}). \tag{9.11}$$

The linear response functions Ω and E are then defined by

$$\Pi(z,\mathbf{q}) = \Omega(z,q)\zeta(z,\mathbf{q}), \qquad \Pi^{(s)}(z,\mathbf{q}) = E(z,q)\hat{\gamma}^{(s)}(z,\mathbf{q}). \tag{9.12}$$

Note that Ω and E are perfectly well-defined once a given solution of (9.9) has been specified (the normalisation of the solution does not matter for this purpose). From (9.9), the response functions satisfy

$$0 = \dot{\Omega} + \frac{1}{2a^3\varepsilon}\Omega^2 - 2\sigma a\varepsilon q^2, \qquad 0 = \dot{E} + \frac{4}{a^3}E^2 - \frac{\sigma a}{4}q^2. \tag{9.13}$$

To deal with holographic non-Gaussianities one must extend the above definition of response functions to quadratic order in perturbation theory [36, 37]. The linear response functions Ω and E are however sufficient to derive the holographic power spectra, as is our goal here.

9.2.3 The Domain-Wall/Cosmology Correspondence

Defining the analytically continued variables $\bar{\kappa}$ and $\bar{q}$ according to

$$\bar{\kappa}^2 = -\kappa^2, \qquad \bar{q} = -iq, \tag{9.14}$$

where $q = +\sqrt{q^2}$ and $\bar{q} = +\sqrt{\bar{q}^2}$ denote *magnitudes* of spatial 3-momenta, it is easy to see that a perturbed cosmological solution written in terms of the variables κ and q continues to a perturbed Euclidean domain-wall solution expressed in terms of the variables $\bar{\kappa}$ and $\bar{q}$. The first continuation is equivalent to reversing the sign of the potential in the background equation of motion (9.7). (We will see shortly, however, that the continuation we have chosen has a clearer interpretation in terms of the variables of the dual QFT.) The second of these analytic continuations generates the necessary sign change $\bar{q}^2 = -q^2$ in the linear equations of motion (9.9). The choice of branch cut we made (i.e., $\bar{q} = -iq$ rather than $\bar{q} = +iq$) stems from the necessity of mapping the cosmological Bunch-Davies vacuum behaviour at early times,

$$\zeta, \hat{\gamma}^{(s)} \sim \exp(-iq\tau) \quad \text{as } \tau = \int^z \frac{\mathrm{d}z'}{a(z')} \to -\infty, \tag{9.15}$$

to the domain-wall solution that decays smoothly in the domain-wall interior,

$$\zeta, \hat{\gamma}^{(s)} \sim \exp(\bar{q}\tau) \quad \text{as } \tau \to -\infty,$$

as required in the calculation of holographic correlation functions.

Turning now to the linear response functions, if we choose $\Omega(z,q)$ and $E(z,q)$ to be cosmological response functions solving (9.13) with $\sigma=-1$ and Bunch-Davies initial conditions, then the corresponding domain-wall response functions $\bar{\Omega}(z,\bar{q})$ and $\bar{E}(z,\bar{q})$ are given by the analytic continuation

$$\bar{\Omega}(z,-iq)=\Omega(z,q),\qquad \bar{E}(z,-iq)=E(z,q). \tag{9.16}$$

(Note we have defined our response functions so that they are independent of κ^2; this was in fact our motivation for introducing the extra factor of κ^2 in (9.10).)

We have thus established that the correspondence between cosmologies and domain-walls holds, not only for the background solutions, but also for linear perturbations around them. This is the basis for the relation between power spectra and holographic 2-point functions, to be discussed shortly. The correspondence also holds at higher order in perturbation theory, allowing cosmological non-Gaussianities to be related to holographic higher-point functions. This may be established in a straightforward fashion by working out the momentum-space Lagrangian for ζ and $\hat{\gamma}^{(s)}$ at higher order in perturbation theory (for explicit results at cubic order, see [36, 37]). One finds that the sign σ is always associated with factors of momenta such that the continuation (9.14) indeed maps perturbed cosmological solutions to perturbed domain-wall solutions.

Finally, let us note the analytic continuations (9.14) may equivalently be expressed in terms of dual QFT variables as

$$\bar{N}=-iN,\qquad \bar{q}=-iq, \tag{9.17}$$

where $\bar{N}$ is the rank of the gauge group of the QFT dual to the domain-wall spacetime, and N is the rank of the gauge group of the *pseudo-QFT* dual to the corresponding cosmology. These relations follow directly from (9.14) noting that in the standard holographic dictionary $\bar{\kappa}^{-2}\propto\bar{N}^2$, working in units where the AdS radius has been set to unity. (Indeed, in our later results, we will see explicitly that holographic correlation functions calculated from the gravity side of the correspondence appear with an overall prefactor of $\bar{\kappa}^{-2}$. On the QFT side of the correspondence, this prefactor corresponds to the overall prefactor of $\bar{N}^2$ in correlators arising from the trace over gauge indices.) Our choice of branch cut in the continuation of $\bar{N}$ has been chosen so that the dimensionless effective QFT coupling, $g^2_{\rm eff}=g^2_{\rm YM}\bar{N}/\bar{q}=g^2_{\rm YM}N/q$, does not change when we analytically continue from QFT to pseudo-QFT. As we will see later in Sect. 9.4.2, this will turn out to be important because the QFT correlators are in general non-analytic functions of $g^2_{\rm eff}$ at large N [2, 19].

9.2.4 Cosmological Power Spectra

In the inflationary paradigm, cosmological perturbations originate on sub-horizon scales as quantum fluctuations of the vacuum. Quantising the interaction picture fields ζ and $\hat{\gamma}_{ij}$ in standard fashion (see, e.g., [28]),

$$\zeta(z,\mathbf{q}) = a(\mathbf{q})\zeta_q(z) + a^\dagger(-\mathbf{q})\zeta_q^*(z), \tag{9.18}$$

$$\hat{\gamma}^{(s)}(z,\mathbf{q}) = b^{(s)}(\mathbf{q})\hat{\gamma}_q(z) + b^{(s)\dagger}(-\mathbf{q})\hat{\gamma}_q^*(z), \tag{9.19}$$

where the creation and annihilation operators obey the usual commutation relations

$$\big[a(\mathbf{q}), a^\dagger(\mathbf{q}')\big] = (2\pi)^3\delta(\mathbf{q}-\mathbf{q}'), \qquad \big[b^{(s)}(\mathbf{q}), b^{(s')\dagger}(\mathbf{q}')\big] = (2\pi)^3\delta(\mathbf{q}-\mathbf{q}')\delta^{ss'}, \tag{9.20}$$

and the mode functions $\zeta_q(z)$ and $\hat{\gamma}_q(z)$ are solutions of the linearised equations of motion (9.9), with initial conditions corresponding to the Bunch-Davies vacuum (9.15). The normalisation of the mode functions is fixed by imposing the canonical commutation relations,[3]

$$\big[\zeta(z,\mathbf{q}), \kappa^{-2}\Pi(z,\mathbf{q}')\big] = i(2\pi)^3\delta(\mathbf{q}+\mathbf{q}'), \tag{9.21}$$

$$\big[\hat{\gamma}_{ij}(z,\mathbf{q}), \kappa^{-2}\Pi_{kl}(z,\mathbf{q}')\big] = i(2\pi)^3\delta(\mathbf{q}+\mathbf{q}')\Pi_{ijkl}, \tag{9.22}$$

where the latter, upon converting to the helicity basis using (9.5), reads

$$\big[\hat{\gamma}^{(s)}(z,\mathbf{q}), \kappa^{-2}\Pi^{(s')}(z,\mathbf{q}')\big] = \frac{i}{2}(2\pi)^3\delta(\mathbf{q}+\mathbf{q}')\delta^{ss'}. \tag{9.23}$$

Using (9.10)–(9.11) and the mode decompositions (9.18)–(9.19), the canonical commutation relations are equivalent to the Wronskian relations

$$i = 2\varepsilon a^3\kappa^{-2}\big(\zeta_q(z)\dot{\zeta}_q^*(z) - \dot{\zeta}_q(z)\zeta_q^*(z)\big), \tag{9.24}$$

$$\frac{i}{2} = \frac{1}{4}a^3\kappa^{-2}\big(\hat{\gamma}_q(z)\dot{\hat{\gamma}}_q^*(z) - \dot{\hat{\gamma}}_q(z)\hat{\gamma}_q^*(z)\big). \tag{9.25}$$

As well as fixing the normalisation of the mode functions, these relations imply

$$\big|\zeta_q(z)\big|^2 = \frac{-\kappa^2}{2\,\mathrm{Im}[\Omega(z,q)]}, \qquad \big|\hat{\gamma}_q(z)\big|^2 = \frac{-\kappa^2}{4\,\mathrm{Im}[E(z,q)]}, \tag{9.26}$$

where we have used the definition of the response functions Ω and E given in (9.12).

Computing now the 2-point functions, we find

$$\big\langle\!\big\langle\zeta(z,q)\zeta(z,-q)\big\rangle\!\big\rangle = \big|\zeta_q(z)\big|^2, \qquad \big\langle\!\big\langle\hat{\gamma}^{(s)}(z,q)\hat{\gamma}^{(s')}(z,-q)\big\rangle\!\big\rangle = \big|\hat{\gamma}_q(z)\big|^2\delta^{ss'}, \tag{9.27}$$

[3] Recall that $\kappa^{-2}\Pi$ and $\kappa^{-2}\Pi^{(s)}$, rather than Π and $\Pi^{(s)}$, are the actual canonical momenta.

where our double bracket notation indicates dropping the delta function associated with momentum conservation, e.g.,

$$\langle z(z,\mathbf{q})\zeta\left(z,\mathbf{q}'\right)\rangle = (2\pi)^3\delta\left(\mathbf{q}+\mathbf{q}'\right)\langle\langle\zeta(z,q)\zeta(z,-q)\rangle\rangle. \tag{9.28}$$

According to convention, the late-time scalar and tensor power spectra are then defined as

$$\Delta_S^2(q) \equiv \frac{q^3}{2\pi^2}\langle\langle\zeta(q)\zeta(-q)\rangle\rangle = \frac{q^3}{2\pi^2}|\zeta_{q(0)}|^2, \tag{9.29}$$

$$\Delta_T^2(q) \equiv \frac{q^3}{2\pi^2}\langle\langle\hat{\gamma}_{ij}(q)\hat{\gamma}_{ij}(-q)\rangle\rangle = \frac{2q^3}{\pi^2}|\hat{\gamma}_{q(0)}|^2, \tag{9.30}$$

where $\zeta_{q(0)}$ and $\hat{\gamma}_{q(0)}$ are the constant late-time values of the cosmological mode functions. Physically, the power spectra represent the contribution to the field variance in position space per logarithmic interval in wavenumbers, e.g.,

$$\langle\zeta(\mathbf{x})^2\rangle = \int\frac{1}{(2\pi)^3}\left(4\pi q^2\mathrm{d}q\right)\langle\langle\zeta(q)\zeta(-q)\rangle\rangle = \int\Delta_S^2(q)\mathrm{d}\ln q.$$

Using (9.26), the cosmological power spectra may also be expressed in terms of the late-time values $\Omega_{(0)}$ and $E_{(0)}$ of the response functions:

$$\Delta_S^2(q) = -\frac{\kappa^2 q^3}{4\pi^2\,\mathrm{Im}[\Omega_{(0)}(q)]}, \qquad \Delta_T^2(q) = -\frac{\kappa^2 q^3}{2\pi^2\,\mathrm{Im}[E_{(0)}(q)]}. \tag{9.31}$$

We will see shortly that the holographic 2-point functions for the corresponding domain-wall spacetime may similarly be expressed in terms of the domain-wall linear response functions. Since the domain-wall response functions are related to the cosmological response functions via (9.16), we will therefore be able to relate the cosmological power spectra above to the holographic 2-point functions.

9.3 Holography for Cosmology

In the present section we turn our attention to the top half of Fig. 9.1, depicting standard gauge/gravity duality. We begin by enumerating the well understood classes of holographic RG flows and discussing some basic features of holographic dualities. We then review Hamiltonian holographic renormalisation and a useful decomposition of the stress tensor 2-point function. Proceeding with our main holographic analysis, we obtain expressions for the stress tensor 2-point function in terms of the domain-wall response functions. Ultimately, our purpose is to derive the holographic formulae for the cosmological power spectra given in (9.66). Readers not

concerned with the more intricate aspects of holographic analysis may prefer to begin with Sects. 9.3.1 and 9.3.2 then skip to Sect. 9.3.6.

9.3.1 Background Solutions

At present, there are two general classes of domain-wall solutions for which a well understood holographic description exists. We list these classes below: it is for these backgrounds that our holographic framework for cosmology is most readily applicable.

(i) *Asymptotically AdS domain-walls*. In this case the solution behaves asymptotically as

$$a(z) \sim e^z, \qquad \varphi \sim 0 \quad \text{as } z \to \infty.$$

The boundary theory has a UV fixed point which corresponds to the bulk AdS critical point. Depending on the rate at which φ approaches zero as $z \to \infty$, the QFT is either a deformation of the conformal field theory (CFT), or else the CFT in a state in which the dual scalar operator acquires a nonvanishing vacuum expectation value (see [43] for details). Under the domain-wall/cosmology correspondence, these solutions are mapped to cosmologies that are asymptotically de Sitter at late times.

(ii) *Asymptotically power-law solutions*. In this case the solution behaves asymptotically as

$$a(z) \sim (z/z_0)^n, \qquad \varphi \sim \sqrt{2n}\log(z/z_0) \quad \text{as } z \to \infty, \tag{9.32}$$

where $z_0 = n-1$. Examples of such dualities are provided by considering the near-horizon limit of the non-conformal branes [5, 18]. In particular, for the case $n = 7$, the asymptotic geometry corresponds to the near-horizon limit of a stack of D2 brane solutions. The detailed holographic dictionary for these theories has been worked out only relatively recently [23, 24, 52]. These theories are characterised by the fact that they have a 'generalised conformal structure' [20–22, 24] (see also Sect. 9.4.1). Under the domain-wall/cosmology correspondence, asymptotically power-law domain walls are mapped to cosmologies that are asymptotically power-law at late times.

9.3.2 Basics of Holography

Gauge/gravity duality is an exact equivalence between a bulk gravitational theory and a boundary QFT. Typically, the boundary QFT is a gauge theory that admits a large-N expansion. The N here denotes the rank of the gauge group: an example of such theory, with gauge group $SU(N)$, is discussed in Sect. 9.4.1. The large-N limit

consists of taking $N \to \infty$ while keeping the 't Hooft coupling $\lambda = g_{YM}^2 N$ fixed. One can show that in this limit only planar diagrams survive [48]. On the bulk side, taking the large-N limit means that one suppresses loop effects. The value of λ then controls whether the supergravity approximation is valid or not.

Under the duality, bulk fields are related to local gauge-invariant operators of the boundary QFT. In particular, the bulk metric is related to the boundary stress tensor, T_{ij}, while bulk scalar fields, such as the inflaton, correspond to boundary scalar operators (e.g., $\mathrm{tr}\, F_{ij} F^{ij}$ where F_{ij} is the gauge field strength and the trace runs over the gauge group indices). More precisely, the map is specified as follows. First, recall that in order to define a quantum theory we must specify the behaviour of the fields at infinity. In a gravitational theory, this means in particular that the spacetime asymptotics must be prescribed. In gauge/gravity duality, the fields that specify the boundary conditions on the bulk side are identified with the sources of the boundary QFT operators [16, 53]. Correlation functions for these gauge-invariant operators may then be extracted from the asymptotics of bulk solutions. Conversely, given the correlation functions of dual operators, one may reconstruct the bulk asymptotics.

Thus, to define the bulk theory, we need to specify appropriate boundary conditions. These boundary conditions must involve an arbitrary boundary metric, since this will act as a source for the stress tensor. Such boundary conditions are supplied by giving an asymptotically locally AdS metric, which in four dimensions takes the form,

$$\begin{aligned} \mathrm{d}s^2 &= \mathrm{d}r^2 + g_{ij}(r,x)\mathrm{d}x^i \mathrm{d}x^j, \\ g_{ij}(r,x) &= e^{2r}\left(g_{(0)ij}(x) + e^{-2r} g_{(2)ij}(x) + \cdots + e^{-2mr} g_{(2m)ij}(x) + \cdots\right). \end{aligned} \tag{9.33}$$

This encompasses the boundary conditions for the bulk metric, both for asymptotically AdS domain-walls and for asymptotically power-law solutions. In the former case, the radial coordinate r may be identified with z, and $2m = 3$. For asymptotically power-law solutions, one may perform a conformal transformation to the *dual frame* [5] defined by $\tilde{g}_{ij} = \exp(-\lambda\Phi) g_{ij}$, where $\lambda = \sqrt{2/n}$. The asymptotic solution above then describes the most general asymptotics for the dual frame metric $\tilde{g}_{ij}$, where now $2m = (3n-1)/(n-1) > 3$ and $r = \int \exp(-\lambda\Phi/2)\mathrm{d}z$ (see [24] for details). In general, much of the holographic analysis for spacetimes with power-law asymptotics may be obtained from that for asymptotically AdS_{2m+1} spacetimes, which are related to power-law spacetimes via dimensional reduction on a T^{2m-3} torus followed by an analytic continuation in m [23].

In the asymptotic expansion (9.33), the leading coefficient $g_{(0)ij}(x)$ is an arbitrary (non-degenerate) three-dimensional metric on the conformal boundary of the bulk spacetime. Since this is the metric on which the dual QFT lives, $g_{(0)ij}$ acts as the source for the dual stress tensor T_{ij}. The subleading coefficients $g_{(2k)ij}(x)$, with $k < m$, are then locally determined in terms of $g_{(0)ij}$ via an asymptotic analysis of the field equations. The coefficient $g_{(2m)ij}(x)$, however, is only partially constrained by this asymptotic analysis. (On the QFT side, these constraints correspond to the QFT Ward identities.) In fact, one finds that the coefficient $g_{(2m)ij}(x)$ is directly

related to the expectation value of the boundary stress tensor [11, 24]:

$$\langle T_{ij} \rangle = \frac{1}{2\bar{\kappa}^2}(2m g_{(2m)ij}). \tag{9.34}$$

An analogous relation also exists for the expectation value of the dual scalar operator in terms of the asymptotic behaviour of the bulk scalar field (see [11, 24] for details). We emphasize that this result only requires that Einstein equations hold asymptotically.

Here, we focused our discussion on the stress tensor, but an analogous discussion holds for all operators provided we specify appropriate boundary conditions for the corresponding bulk fields. If one includes such additional fields, then the holographic formulae such as (9.34) will in general acquire additional terms [3, 4], but the structure described above remains the same. More importantly for our purposes, since we are only interested in correlation functions of the stress tensor, we only need to turn on a source for the stress tensor, in which case the formulae above hold unchanged.[4]

The relation (9.34) may be read in two ways: (i) given a bulk gravitational solution we may read off the dual QFT data encoded by the solution; (ii) given QFT data we may reconstruct the bulk asymptotic solution. We stress that this asymptotic reconstruction is possible even when gravity is strongly coupled in the interior (corresponding to a weakly coupled boundary QFT). The coefficients up to $g_{(2m)ij}$ simply encode the boundary conditions, i.e., the fact that we are considering asymptotically locally AdS configurations (in the dual frame for the power-law case). In gauge/gravity duality, these terms encode the fact that we have turned on a source for the dual operator (the stress tensor for the case at hand), and this is unrelated to whether the dual QFT is at weak or strong coupling. The first term to depend on the bulk dynamics is $g_{(2m)ij}$. When gravity is weakly coupled, this coefficient is determined by the behaviour of the gravitational solution deep in the interior. When gravity is strongly coupled, this coefficient should be obtained by solving the full stringy dynamics in the interior. Gauge/gravity duality requires that the value obtained this way *must agree* with the $g_{(2m)ij}$ determined via (9.34) from the weakly coupled dual QFT.

9.3.3 Hamiltonian Holographic Renormalisation

In the following, rather than using (9.34) directly, we will instead employ the radial Hamiltonian formulation of [38, 39]. Here, the radial direction plays a role equivalent to that of time in the usual Hamiltonian formalism. The radial Hamiltonian formulation has a number of advantages for our present purposes; in particular, it

[4] Modulo contributions to (9.34) from condensates of low-dimension operators, cf. the discussion of the Coulomb branch flow in [3, 4]. Such cases can be analysed along similar lines but we will not discuss this here.

leads to a universal formula for the 1-point function that is independent of any of the issues (additional fields, etc.) discussed in the previous subsection. It further permits us to work with an arbitrary potential for the scalar field, so long as this potential admits background solutions of either the asymptotically AdS or the asymptotically power-law form. (In contrast, the formula (9.34) must be established on a case by case basis for different potentials, as in [3, 4, 11].)

A key feature of spacetimes of the form (9.33) is that, to leading order as $r \to \infty$, the radial derivative is equal to the dilatation operator δ_D, i.e.,

$$\partial_r = \delta_D\left(1 + O\left(e^{-2r}\right)\right), \tag{9.35}$$

where the δ_D acts on the metric as $\delta_D g_{ij}(x, r) = 2g_{ij}(x, r)$. (In particular, this means the scale factor a transforms as $\delta_D a = a$.) The bulk scalar field also transforms with a specific conformal weight. Equation (9.35) is a sharp version of the oft-quoted relation between the radial direction and the energy scale of the dual QFT. This equivalence allows one to trade the asymptotic radial expansion (9.33) for a covariant expansion in eigenfunctions of the dilatation operator. By definition, an eigenfunction $A_{(n)}$ of weight n satisfies

$$\delta_D A_{(n)} = -nA_{(n)},$$

hence, for example, the scale factor a has weight minus one. From (9.35), $A_{(n)} \sim e^{-nr}(1 + O(e^{-2r}))$, so the radial expansion and the expansion in eigenfunctions of the dilatation operator are closely related. The latter expansion is manifestly covariant, however, whereas expanding in the bulk radial coordinate is not a covariant operation.

In the radial Hamiltonian formalism then, the expectation value of the dual stress tensor is given by

$$\langle T^i_j \rangle = \left(\frac{-2}{\sqrt{g}}\Pi^i_j\right)_{(3)} \tag{9.36}$$

where Π^i_j is the radial canonical momentum in Fefferman-Graham gauge where $N_i = 0$ and $N = 1$, and the subscript indicates taking the piece with overall dilatation weight three.[5] Indeed, one might have anticipated this on general grounds, since in three dimensions the conformal dimension of the stress tensor is three. Equation (9.36) is the universal formula we mentioned above.[6] To extract the piece with

[5] In odd bulk dimensions the transformation of this specific coefficient also has an additional anomalous contribution due to the conformal anomaly [17]. In four bulk dimensions there is no anomaly, however, and this coefficient is a true eigenfunction of δ_D.

[6] Strictly speaking, while (9.36) holds universally, expressing Π^i_j in terms of the coefficients in the asymptotic expansion of the bulk fields depends on the details of theory under consideration (field content, interactions, etc.). Fortunately, however, we will not need this information here.

dilatation weight three, Π^i_j may first be decomposed in eigenfunctions of the dilatation operator. In general, the radial canonical momentum will contain pieces with weight less than three: the process of holographic renormalisation then amounts to determining these terms through the asymptotic analysis and subtracting them. In [38, 39], it is shown that removing these pieces is equivalent to adding local boundary covariant counterterms to the on-shell action.

For asymptotically AdS domain-walls, the radial canonical momentum is

$$\Pi^i_j = \frac{1}{2\bar{\kappa}^2}\sqrt{g}\big(K^i_j - K\delta^i_j\big), \tag{9.37}$$

where $K_{ij} = (1/2)\partial_z g_{ij}$ is the extrinsic curvature of constant-z slices. (Recall for domain-walls, the z coordinate is a radial variable.) In the case of asymptotically power-law domain-walls, the relevant radial canonical momentum is instead that of the dual frame [24], namely

$$\tilde{\Pi}^i_j = \frac{1}{2\bar{\kappa}^2}\sqrt{\tilde{g}}e^{\lambda\Phi}\big(\tilde{K}^i_j - (\tilde{K} + \lambda\Phi_{,r})\delta^i_j\big). \tag{9.38}$$

Here, all tilded quantities belong to the dual frame and $\partial_r = e^{\lambda\varphi/2}\partial_z$. (Note the r.h.s. of (9.36) should also be evaluated in the dual frame.)

9.3.3.1 Constraint Equations

In our later analysis, we will need to make use of the Hamiltonian and momentum constraint equations, and so it is convenient to first present these here. As mentioned above, for asymptotically AdS domain-walls, the holographic analysis is performed in Fefferman-Graham gauge with $N = 1$ and $N_i = 0$. In the case of asymptotically power-law domain-walls, the holographic analysis also requires the choice of Fefferman-Graham gauge, but in the *dual frame*. The corresponding Einstein frame metric $g_{ij} = e^{\lambda\Phi}\tilde{g}_{ij}$ then has vanishing shift N_i but a nonzero lapse perturbation $\delta N = (\lambda/2)\delta\varphi$. In the following, to cover both cases, we will assume the shift has been gauged to zero but allow for a nonzero lapse perturbation.

Differentiating the Lagrangian (9.6) with respect to N and N_i, we obtain the domain-wall Hamiltonian and momentum constraints

$$0 = -R + K^2 - K_{ij}K^{ij} + 2\bar{\kappa}^2 V - N^{-2}\dot{\Phi}^2 + g^{ij}\Phi_{,i}\Phi_{,j}, \tag{9.39}$$

$$0 = \nabla_j\big(K^j_i - \delta^j_i K\big) - N^{-1}\dot{\Phi}\Phi_{,i}, \tag{9.40}$$

where $K_{ij} = (1/2N)\dot{g}_{ij}$. Expanding to linear order then yields

$$0 = -4a^{-2}\partial^2\psi + 2H\dot{h} + 4\bar{\kappa}^2 V\delta N - 2\dot{\varphi}\delta\dot{\varphi} + 2\bar{\kappa}^2 V'\delta\varphi, \tag{9.41}$$

$$0 = \frac{1}{2}\dot{h}_{ij,j} - \frac{1}{2}\dot{h}_{,i} + 2H\delta N_{,i} - \dot{\varphi}\delta\varphi_{,i}. \tag{9.42}$$

Acting on the latter equation with $\partial^{-2}\partial_i$ we may extract the scalar part

$$0 = 2\dot{\psi} - \dot{\varphi}\delta\varphi + 2H\delta N. \tag{9.43}$$

9.3.4 The Stress Tensor 2-Point Function

Prior to commencing our holographic calculation, let us briefly discuss the QFT correlator that will be of interest to us, the stress tensor 2-point function. As we have in mind some regular three-dimensional QFT dual to a domain-wall spacetime, we will denote momenta using $\bar{\mathbf{q}}$ rather than $\mathbf{q}$. The boundary metric on which the QFT lives will moreover be flat in the absence of sources.

Quite generally, the diffeomorphism Ward identity implies that the stress tensor 2-point function is transverse, i.e.,

$$0 = \bar{q}_i \langle\!\langle T_{ij}(\bar{q}) T_{kl}(-\bar{q}) \rangle\!\rangle.$$

Our double bracket notation here once again suppresses the delta function associated with momentum conservation, as in (9.28). It is then a simple exercise to show that only two transverse tensors with the correct symmetries can be built from the momentum $\bar{q}_i$ and the background metric δ_{ij}. Through this argument, we find the stress tensor 2-point function admits the general decomposition

$$\langle\!\langle T_{ij}(\bar{q}) T_{kl}(-\bar{q}) \rangle\!\rangle = A(\bar{q}) \Pi_{ijkl} + B(\bar{q}) \pi_{ij} \pi_{kl}. \tag{9.44}$$

Here, $A(\bar{q})$ encodes the transverse traceless piece of the 2-point function while $B(\bar{q})$ encodes the trace piece, since

$$\langle\!\langle T^{(s)}(\bar{q}) T^{(s')}(-\bar{q}) \rangle\!\rangle = \frac{1}{2} A(\bar{q}) \delta^{ss'}, \qquad \langle\!\langle T(\bar{q}) T(-\bar{q}) \rangle\!\rangle = 4B(\bar{q}),$$

where $T^{(s)}(\bar{\mathbf{q}}) = (1/2)\varepsilon_{ij}^{(s)}(-\bar{\mathbf{q}}) T_{ij}(\bar{\mathbf{q}})$ in parallel with our earlier treatment of $\hat{\gamma}^{(s)}(\bar{\mathbf{q}})$.

At a more formal level, the 2-point function encodes the variation of the 1-point function in the presence of sources, $\delta\langle T^i_j \rangle_s$, under a linear variation of the appropriate source, in this case the metric $g_{(0)ij}$ on which the QFT lives. Setting $g_{(0)ij} = \delta_{ij} + \delta g_{(0)ij}$, we therefore have

$$\delta\langle T^i_j(\mathbf{x}) \rangle_s = \delta^{im} \delta\langle T_{mj}(\mathbf{x}) \rangle_s = -\frac{1}{2} \int \mathrm{d}\mathbf{x}' \delta^{im} \langle T_{mj}(\mathbf{x}) T_{kl}(\mathbf{x}') \rangle\!\rangle \delta g^{kl}_{(0)}(\mathbf{x}'),$$

where in the first equality we used the fact that the 1-point function $\langle T_{ij}(\mathbf{x})\rangle$ vanishes on a flat background (i.e., with the source set to zero). In momentum space, this becomes

$$\delta\langle T^i_j(\bar{\mathbf{q}})\rangle = -\frac{1}{2}\delta^{im}\langle\langle T_{mj}(\bar{q})T_{kl}(-\bar{q})\rangle\rangle\delta g^{kl}_{(0)}(\bar{\mathbf{q}}).$$

In particular, inserting (9.44) and decomposing the metric variation as in (9.3), we find

$$\delta\langle T^{(s)}(\bar{\mathbf{q}})\rangle_s = \frac{1}{2}A(\bar{q})\gamma^{(s)}_{(0)}(\bar{\mathbf{q}}), \qquad \delta\langle T(\bar{\mathbf{q}})\rangle_s = -4B(\bar{q})\psi_{(0)}(\bar{\mathbf{q}}). \tag{9.45}$$

9.3.5 Holographic Analysis

Our goal is now to evaluate the stress tensor 2-point function in terms of the domain-wall response functions. To do so, we will expand (9.36) to linear order in the sources then compare with (9.45). We will deal first of all with the case of asymptotically AdS domain-walls before turning to the case of power-law asymptotics.

Working in Fefferman-Graham gauge where $N = 1$ and $N_i = 0$, expanding out (9.37) in momentum space to linear order, we find

$$\delta\langle T^{(s)}\rangle_s = -\frac{1}{2}\bar{\kappa}^{-2}\dot{\gamma}^{(s)}_{(3)}, \qquad \delta\langle T\rangle_s = \bar{\kappa}^{-2}\dot{h}_{(3)}. \tag{9.46}$$

Substituting for $\dot{\gamma}^{(s)}$ using (9.11)–(9.12), the first of these equations reads

$$\delta\langle T^{(s)}\rangle_s = -2\bar{\kappa}^{-2}\big[a^{-3}\bar{E}(\bar{q})\gamma^{(s)}\big]_{(3)}.$$

As the factor a^{-3} has dilation weight three, the coefficient of the source $\gamma^{(s)}_{(0)}$ is $-2\bar{\kappa}^{-2}\bar{E}_{(0)}(\bar{q})$. Comparing with (9.45), we may then identify the transverse traceless piece of the 2-point function,

$$A(\bar{q}) = -4\bar{\kappa}^{-2}\bar{E}_{(0)}(\bar{q}). \tag{9.47}$$

In this formula, the zero subscript indicates taking the piece of the response function that has zero weight under dilatations, i.e., the piece that is independent of r as $r \to \infty$. In general, $\bar{E}$ diverges as $r \to \infty$, and so to extract $\bar{E}_{(0)}$ correctly requires first determining the terms with eigenvalue less than zero and subtracting these from $\bar{E}$, before taking the limit $r \to \infty$ (see the example in the next subsection, and also [39]). The issue here is that the subtraction of the infinite pieces may induce a change in the finite part as well, which may happen if the local covariant counterterms needed to cancel the infinities necessarily have a finite part as well.

To identify the trace piece $B(\bar{q})$ of the stress tensor 2-point function we need to express $\dot{h}$ in terms of ψ, which requires use of the constraint equations. Setting $\delta N = 0$, the Hamiltonian and momentum constraints (9.41) and (9.43) take the form

$$\dot{h} = -\frac{2\bar{q}^2}{a^2 H}\psi + \frac{\dot{\varphi}}{H}\delta\dot{\varphi} + (\ldots)\delta\varphi, \qquad \dot{\psi} = (\ldots)\delta\varphi. \tag{9.48}$$

Here, and in the following, we will ignore terms proportional to $\delta\varphi$ since these do not contribute to $B(\bar{q})$. (Instead, since $\delta\phi_{(0)}$ sources the dual scalar operator O, they contribute to the correlator $\langle T\,O\rangle$.) Now, on the one hand, we have

$$\dot{\zeta} = \left(-\psi - \frac{H}{\dot{\varphi}}\delta\dot{\varphi}\right) = -\frac{H}{\dot{\varphi}}\delta\dot{\varphi} + (\ldots)\delta\varphi, \tag{9.49}$$

while on the other hand,

$$\dot{\zeta} = \frac{1}{2a^3\varepsilon}\Pi = \frac{1}{2a^3\varepsilon}\bar{\Omega}(\bar{q})\zeta = -\frac{1}{2a^3\varepsilon}\bar{\Omega}(\bar{q})\psi + (\ldots)\delta\varphi. \tag{9.50}$$

Thus, at linear order,

$$\delta\dot{\varphi} = \frac{H}{a^3\dot{\varphi}}\bar{\Omega}(\bar{q})\psi + (\ldots)\delta\varphi, \qquad \dot{h} = \left(\frac{\bar{\Omega}(\bar{q})}{a^3} - \frac{2\bar{q}^2}{a^2 H}\right)\psi + (\ldots)\delta\varphi. \tag{9.51}$$

From (9.46) and (9.45), we then identify

$$B(\bar{q}) = -\frac{1}{4}\bar{\kappa}^{-2}\bar{\Omega}_{(0)}. \tag{9.52}$$

Note we have dropped the contribution to $B(\bar{q})$ from the term in (9.51) proportional to $\bar{q}^2$: this contribution simply amounts to a scheme-dependent contact term which may be removed through the addition of a finite local counterterm. In extracting the zero-dilatation weight piece of the response function $\bar{\Omega}_{(0)}$, similar considerations apply as discussed above for the case of $\bar{E}_{(0)}$.

Having seen how the stress tensor 2-point function for asymptotically AdS domain-walls is given by the zero-dilatation weight pieces of the appropriate response functions, let us now turn to the case of asymptotically power-law domain-walls. Fortunately the analysis is very closely related to that above. We start by writing the perturbed dual frame metric in Fefferman-Graham gauge as

$$\mathrm{d}\tilde{s}^2 = e^{-\lambda\Phi}\mathrm{d}s^2 = \mathrm{d}r^2 + \tilde{a}^2[\delta_{ij} + \tilde{h}_{ij}]\mathrm{d}x^i\mathrm{d}x^j, \tag{9.53}$$

$$\tilde{h}_{ij} = -2\tilde{\psi}\delta_{ij} + 2\tilde{\chi}_{,ij} + 2\tilde{\omega}_{(i,j)} + \tilde{\gamma}_{ij}, \tag{9.54}$$

where $\tilde{a} = ae^{-\lambda\varphi/2}$ and $\mathrm{d}r = e^{-\lambda\varphi/2}\mathrm{d}z$. These dual frame perturbations are then related to their Einstein frame counterparts by

$$\tilde{\psi} = \psi + (\lambda/2)\delta\varphi, \qquad \tilde{\chi} = \chi, \qquad \tilde{\omega}_i = \omega_i, \qquad \tilde{\gamma}_{ij} = \gamma_{ij}.$$

In addition, we have a nonzero Einstein frame lapse perturbation $\delta N = (\lambda/2)\delta\varphi$ as noted previously.

The 1-point function in the presence of sources is given by (9.36), using the dual frame canonical momentum (9.38). Expanding (9.38) to linear order and converting dual frame perturbations to Einstein frame perturbations (as well as r-derivatives to z-derivatives), we obtain

$$\delta\langle T^{(s)}\rangle_s = -\frac{1}{2}\bar{\kappa}^{-2}\big[e^{3\lambda\varphi/2}\dot{\gamma}^{(s)}\big]_{(3)}, \qquad \delta\langle T\rangle_s = \bar{\kappa}^{-2}\big[e^{3\lambda\varphi/2}\dot{h} + (\ldots)\delta\varphi\big]_{(3)}.$$

One may now proceed as in the asymptotically AdS case, using the response functions to substitute for the radial derivatives of metric perturbations, the only difference being that there is now a nonzero lapse perturbation. Since the constraint equations (9.41) and (9.43) only involve δN and its spatial derivative $\delta N_{,i}$, but never its radial derivative $\delta\dot{N}$, the new terms involving the lapse perturbation can only contribute to the $(\ldots)\delta\varphi$ piece and never to the piece of interest proportional to ψ. (If there *were* a piece proportional to $\delta\dot{N} = (\lambda/2)\delta\dot{\varphi}$, this would contribute a term proportional to ψ via (9.51).) We may therefore recycle our analysis above giving

$$\delta\langle T^{(s)}\rangle_s = -2\bar{\kappa}^{-2}\big[e^{3\lambda\varphi/2}a^{-3}\bar{E}(\bar{q})\gamma^{(s)}\big]_{(3)}, \tag{9.55}$$

$$\delta\langle T\rangle_s = \bar{\kappa}^{-2}\left[e^{-3\lambda\varphi/2}\left(\frac{\bar{\Omega}(\bar{q})}{a^3} - \frac{2\bar{q}^2}{a^2H}\right)\psi + (\ldots)\delta\varphi\right]_{(3)}. \tag{9.56}$$

Returning to the dual frame,

$$\delta\langle T^{(s)}\rangle_s = -2\bar{\kappa}^{-2}\big[\tilde{a}^{-3}\bar{E}(\bar{q})\tilde{\gamma}^{(s)}\big]_{(3)}, \tag{9.57}$$

$$\delta\langle T\rangle_s = \bar{\kappa}^{-2}\left[\left(\frac{\bar{\Omega}(\bar{q})}{\tilde{a}^3} - \frac{2\bar{q}^2e^{\lambda\varphi/2}}{\tilde{a}^2H}\right)\tilde{\psi} + (\ldots)\delta\varphi\right]_{(3)}. \tag{9.58}$$

Since the dilatation weight of $\tilde{a}$ in the dual frame is minus one, examining the above we in fact recover precisely our previous results (9.47) and (9.52). These results are thus valid for both asymptotically AdS domain-walls as well as for asymptotically power-law domain-walls. In the latter case, however, the subtraction of terms with negative dilatation weight before sending $r \to \infty$ should be performed in the dual frame, as we will see in the following example.

9.3.5.1 An Example: Exact Power-Law Inflation

To illustrate the above discussion, let us consider the domain-wall backgrounds exactly equal (rather than merely asymptotic) to (9.32), namely

$$a = (z/z_0)^n, \qquad \varphi = \sqrt{2n}\ln(z/z_0), \qquad z_0 = n-1 > 0.$$

Under the domain-wall/cosmology correspondence, these solutions are mapped to cosmologies undergoing exact power-law inflation. While this particular model is strongly constrained by the WMAP data [25], this need not concern us here since our purpose is simply to illustrate the steps involved in the holographic computation. Furthermore, we will see in Sect. 9.4 that the strong coupling version of these models (i.e., where gravity is strongly coupled at early times but the dual three-dimensional QFT is weakly coupled) are compatible with observations.

Referring back to the background equations of motion (9.7), we find the function $W = -(2n/z_0)\exp(-\varphi/\sqrt{2n})$. It then follows that $\varepsilon = 1/n$ and both mode functions $\hat{\gamma}_q$ and ζ_q obey the same equation of motion, which for the domain-wall spacetime reads

$$0 = \ddot{\zeta}_{\bar{q}} + (3n/z)\dot{\zeta}_{\bar{q}} - (z/z_0)^{-2n}\bar{q}^2\zeta_{\bar{q}}. \tag{9.59}$$

Imposing regularity in the interior, the solution is

$$\zeta_{\bar{q}} = C_{\bar{q}}\rho^{\sigma}K_{\sigma}(\rho),$$

where K_σ is a modified Bessel function of the second kind of order $\sigma = (3n-1)/2(n-1) > 3/2$, the radial coordinate $\rho = \bar{q}(z/z_0)^{1-n}$, and $C_{\bar{q}}$ is an arbitrary function of $\bar{q}$. The boundary $z \to \infty$ corresponds to $\rho = 0$ while the domain-wall interior corresponds to $\rho \to \infty$. The corresponding radial canonical momentum (times $\bar{\kappa}^2$) is equal to

$$\Pi_{\bar{q}} = \frac{2\varepsilon}{a^3}\dot{\zeta}_{\bar{q}} = -\frac{2C_{\bar{q}}}{n}\left(\frac{\rho}{\bar{q}}\right)^{-2\sigma}\rho\partial_\rho\left(\rho^{\sigma}K_{\sigma}(\rho)\right). \tag{9.60}$$

Expanding about $\rho = 0$, we find

$$\begin{aligned}
\zeta_{\bar{q}} &= C_{\bar{q}}\left(1 + \frac{1}{4(1-\sigma)}\rho^2 + \cdots - \frac{\Gamma(1-\sigma)}{4^{\sigma}\Gamma(1+\sigma)}\rho^{2\sigma} + \cdots\right), \\
\Pi_{\bar{q}} &= -C_{\bar{q}}\frac{2\bar{q}^{2\sigma}}{n}\left(\frac{1}{2(1-\sigma)}\rho^{2(1-\sigma)} + \cdots - \frac{2\sigma\Gamma(1-\sigma)}{4^{\sigma}\Gamma(1+\sigma)} + \cdots\right),
\end{aligned} \tag{9.61}$$

and thus

$$\Omega(\bar{q}) = \frac{\Pi_{\bar{q}}}{\zeta_{\bar{q}}} = -\frac{2\bar{q}^{2\sigma}}{n}\left(\frac{1}{2(1-\sigma)}\rho^{2(1-\sigma)} + \cdots - \frac{2\sigma\Gamma(1-\sigma)}{4^{\sigma}\Gamma(1+\sigma)} + \cdots\right). \tag{9.62}$$

As expected, this diverges as $\rho \to 0$. To compute the 2-point function we need to identify the parts that have negative dilatation eigenvalue, subtract them from (9.62), and then take $\rho \to 0$.

To do this, we first transform to the dual frame via $\tilde{g}_{ij} = e^{-\sqrt{(2/n)}\varphi} g_{ij}$ and then change radial variable, $r = z_0 \ln(z/z_0) = -\ln(\rho/\bar{q})$. The metric is now that of AdS,

$$\mathrm{d}s^2 = \mathrm{d}r^2 + e^{2r}\mathrm{d}\mathbf{x}^2,$$

and the dilatation operator is exactly equal to the radial derivative,

$$\delta_D = \partial_r = -\rho\partial_\rho.$$

(This reflects the fact that the AdS isometry group is the same as the conformal group in one dimension less.) It follows that any monomial in ρ is an eigenfunction of δ_D,

$$\delta_D \rho^n = -n\rho^n,$$

and one can simply identify in (9.62) all terms with negative eigenvalue; for example, $\bar{\Omega}_{(-2\sigma+2)} = -\bar{q}^{2\sigma}\rho^{-2(\sigma-1)}/(n(1-\sigma))$. We then have

$$\bar{\Omega}_{(0)} = \frac{4\sigma\Gamma(1-\sigma)}{n4^\sigma\Gamma(1+\sigma)}\bar{q}^{2\sigma}.$$

In this example, the identification of the terms with negative eigenvalues could be accomplished by inspection. In more complicated examples, however, this is no longer the case, so we briefly indicate here how one could compute them (see [39] for a more complete discussion). Starting from (9.13) with $\sigma = +1$ and changing the radial coordinate from z to r, one obtains

$$\partial_r\bar{\Omega} + \frac{n}{2}\bar{\Omega}^2 e^{-2\sigma r} - \frac{2}{n}\bar{q}^2 e^{2(\sigma-1)r} = 0. \tag{9.63}$$

This equation may now be solved asymptotically by expanding Ω in dilatation eigenvalues,

$$\bar{\Omega} = \sum_{k\geq 1}\bar{\Omega}_{(-2\sigma+2k)},$$

making use[7] of $\partial_r = \delta_D$ and collecting all terms with the same weight. For example, to leading order, at weight $(-2\sigma+2)$, only the first and last term in (9.63) can have this weight, and one obtains $\bar{\Omega}_{(-2\sigma+2)} = -(\bar{q}^2/n(1-\sigma))\exp(2(\sigma-1)r)$ in agreement with our earlier result. Through iteration, one may obtain all coefficients with negative eigenvalue.

[7] In examples where the background solution is only asymptotically AdS, the relation between the dilatation operator and the radial derivative contains subleading terms (see (9.35)) that must be taken into account. For a full discussion, see [39].

Having obtained $\bar{\Omega}_{(0)}$, we finally compute $B(\bar{q})$:

$$B(\bar{q}) = -\frac{1}{4}\bar{\kappa}^{-2}\bar{\Omega}_{(0)} = -\frac{\sigma\,\Gamma(1-\sigma)}{n4^{\sigma}\,\Gamma(1+\sigma)}\bar{\kappa}^{-2}\bar{q}^{2\sigma} = -\frac{\pi}{4^{\sigma}\,\Gamma^2(\sigma)n\sin\pi\sigma}\bar{\kappa}^{-2}\bar{q}^{2\sigma}.$$

A near-identical argument holds for the tensors $\hat{\gamma}^{(s)}$ yielding $\bar{\Omega}_{(0)} = (8/n)\bar{E}_{(0)}$, and hence $A(\bar{q}) = 2nB(\bar{q})$. Via the domain-wall/cosmology correspondence, applying the continuations (9.14), the imaginary parts of the cosmological response functions are

$$\mathrm{Im}\,\Omega_{(0)} = (8/n)\,\mathrm{Im}\,E_{(0)} = -\frac{4\pi}{n4^{\sigma}\,\Gamma^2(\sigma)}\kappa^{-2}q^{2\sigma}. \tag{9.64}$$

From (9.31), we then recover the expected cosmological power spectra:

$$\Delta^2_S(q) = \frac{n}{16}\Delta^2_T(q) = \frac{n4^{\sigma-2}\Gamma^2(\sigma)}{\pi^3}\kappa^2 q^{3-2\sigma}. \tag{9.65}$$

Note that we could equally well have obtained (9.64) by applying the continuations (9.14) to the *unrenormalised* domain-wall response function (9.62), then taking the imaginary part followed by the limit $z \to \infty$. This is because the divergent terms one subtracts to obtain the renormalised response functions are all analytic functions of $\bar{q}^2$ (as may be seen from (9.62), where the leading term is proportional to $\bar{q}^2$) and hence under the continuation $\bar{q}^2 = -q^2$, these terms remain real and do not contribute to the imaginary part of the cosmological response functions. Only the leading *non-analytic* piece of the domain-wall response functions contributes to the late-time imaginary part of the cosmological response functions: this leading non-analytic piece is finite and is simply $\bar{\Omega}_{(0)}$. In fact, the late-time values of the imaginary parts of the cosmological response functions have to be finite as a consequence of the Wronskian relations (9.24)–(9.25) and the fact that ζ and $\hat{\gamma}_{ij}$ tend to finite constants at late times.

9.3.6 Holographic Formulae for the Power Spectra

After the detailed arguments of the preceding subsections, let us summarise our progress thus far. Firstly, in (9.31), we expressed the cosmological power spectra in terms of the imaginary pieces of the cosmological response functions at late times. Secondly, in (9.47) and (9.52), we saw how the stress tensor 2-point function of the dual QFT is given by the zero-dilatation weight pieces of the corresponding domain-wall response functions. To extract these zero-dilatation weight pieces, the domain-wall response functions had first to be renormalised by subtracting counterterms with negative dilatation weight, before sending $z \to \infty$. As we saw in the previous subsection, however, these counterterms are necessarily analytic functions of $\bar{q}^2$, and so do not contribute to the imaginary part of the corresponding cosmological response function at late times. The latter is therefore precisely given by analytically

continuing the zero-dilatation weight piece of the domain-wall response function according to (9.16) and taking the imaginary part. Putting all this together, we arrive at our principal result: that the cosmological power spectra are directly related to the stress tensor 2-point function of the dual QFT via the holographic formulae

$$\Delta_S^2(q) = \frac{-q^3}{16\pi^2 \operatorname{Im} B(-iq)}, \qquad \Delta_T^2(q) = \frac{-2q^3}{\pi^2 \operatorname{Im} A(-iq)}. \tag{9.66}$$

In these formulae, as well as the analytic continuation of momentum indicated, one must also continue $\bar{N} = -iN$. As one might expect, the scalar power spectrum is related to the trace piece of the stress-tensor 2-point function, while the tensor power spectrum is related to the transverse traceless piece of the 2-point function.

9.4 Holographic Phenomenology for Cosmology

As noted in the introduction, one of the most striking features of holographic dualities is that they are strong/weak coupling dualities, meaning that when one description is weakly coupled, the other is strongly coupled, and vice versa. In the regime where the dual QFT is strongly coupled then, the gravitational description is weakly coupled and our holographic formulae should (and indeed they do) reproduce the results of standard single-field inflation. In this situation, application of the holographic framework offers a fresh perspective, and may lead to new insights, but offers no new predictions.

In the regime in which the dual QFT is weakly coupled, however, the corresponding gravitational description is instead *strongly coupled* at very early times. Let us emphasize that by 'strongly coupled' gravity we do *not* mean that the perturbative fluctuations around the background FRW spacetime are strongly coupled, but rather, that the description in terms of metric fluctuations is itself not valid. This is a non-geometric 'stringy' phase. A geometric description emerges only asymptotically, and at late times one recovers a specific accelerating FRW spacetime (to be matched to conventional hot big bang cosmology), along with a specific set of inhomogeneities. Crucially, these inhomogeneities are not linked with a perturbative quantisation around the FRW spacetime as in conventional inflation, but rather, they originate from the dynamics of the dual weakly coupled QFT. Holography thus suggests a natural generalisation of the inflationary mechanism to strongly coupled gravity, in which the properties of cosmological perturbations may be determined through three-dimensional perturbative QFT calculations. To follow these late-time inhomogeneities through the reheating transition to the post-inflationary universe, just as in conventional inflation, one then makes use of the conservation of ζ and $\hat{\gamma}_{ij}$ on superhorizon scales (or more generally, the 'separate universes' argument, see e.g., [8, 42]).

In order to compute the observational predictions of such a scenario, it is necessary to specify more precisely the nature of the dual QFT. Ideally, one would be able to deduce this from first principles via some string/M-theoretic construction. In the absence of such a construction, we will instead pursue a (holographic) phenomenological approach. As with other known holographic dualities, the dual QFT will in general involve scalars, fermions and gauge fields, and it should admit a large N limit. The question is then whether one can find a theory which is compatible with current observations. A further guiding principle is to consider QFTs of the type featured earlier in Sect. 9.3.1, for which the holographic dual is well understood. One might thus consider either deformations of CFTs (dual to asymptotically de Sitter cosmologies) or else QFTs with a generalised conformal structure (dual to asymptotically power-law cosmologies). In the following we will focus on the latter class of QFTs, leaving exploration of the former to future work.

9.4.1 A Prototype Dual QFT

Any QFT dual to an asymptotically power-law cosmology is required to satisfy quite a restrictive set of properties [24]. Specifically, (i) it should admit a large-N limit, (ii) all fields should be massless, (iii) it should have a dimensionful coupling constant, and (iv) all terms in the Lagrangian should have the same scaling dimension, which should be different from three. The properties (ii)–(iv) imply that the theory admits a *generalised conformal structure* [22], i.e., the theory would be conformal if the coupling constant is promoted to a background field transforming non-trivially under conformal transformations.

A simple class of models exhibiting these properties is given by three-dimensional $SU(\bar{N})$ Yang-Mills theory coupled to a number of massless scalars and fermions, all transforming in the adjoint of $SU(\bar{N})$, and with interactions consisting of Yukawa and quartic scalar terms. (We write the rank of the QFT gauge group as $\bar{N}$ here, since we will first be performing calculations using the QFT dual to the domain-wall spacetime before analytically continuing to the pseudo-QFT.) Theories of this type are typical in holography where they appear as the worldvolume theories of D-branes. In three dimensions, the Yang-Mills coupling $g^2_{\rm YM}$ has dimension one and so the theory is super-renormalisable. Moreover, by rescaling the fields appropriately, one may arrange that the coupling appears only as an overall constant multiplying the action. Assigning scaling dimension one to scalars and gauge fields, and $3/2$ to fermions, one finds that kinetic terms and the interactions all have dimension four. Allowing $\mathscr{N}_A$ gauge fields A^I $(I = 1, \ldots, \mathscr{N}_A)$; $\mathscr{N}_\phi$ minimal scalars ϕ^J $(J = 1, \ldots, \mathscr{N}_\phi)$; $\mathscr{N}_\chi$ conformal scalars χ^K $(K = 1, \ldots, \mathscr{N}_\chi)$ and $\mathscr{N}_\psi$ fermions ψ^L $(L = 1, \ldots, \mathscr{N}_\psi)$, the Lagrangian then takes the form

$$S = \frac{1}{g^2_{\rm YM}} \int \mathrm{d}^3x \, \mathrm{tr}\Big[\frac{1}{2} F^I_{ij} F^{Iij} + \frac{1}{2}\big(D\phi^J\big)^2 + \frac{1}{2}\big(D\chi^K\big)^2 + \bar{\psi}^L D\psi^L$$

$$+\lambda_{M_1M_2M_3M_4}\Phi^{M_1}\Phi^{M_2}\Phi^{M_3}\Phi^{M_4}+\mu^{\alpha\beta}_{ML_1L_2}\Phi^{M}\psi^{L_1}_{\alpha}\psi^{L_2}_{\beta}\Big]. \tag{9.67}$$

Here, the couplings $\lambda_{M_1M_2M_3M_4}$ and $\mu^{\alpha\beta}_{ML_1L_2}$ (where α and β are spinor indices) are dimensionless, and we have grouped the scalars appearing in the interaction terms as $\Phi^M=(\{\phi^J\},\{\chi^K\})$. When we couple the theory to gravity, the conformal scalars acquire an additional $R\chi^2$ coupling; on a flat background this means the conformal scalars have a different stress tensor to their minimally coupled counterparts. Specifically, the stress tensor on a flat background is given by

$$\begin{aligned}T_{ij}=\frac{1}{g^2_{\mathrm{YM}}}\,\mathrm{tr}\Big[&2F^I_{ik}F^{Ik}_j+D_i\phi^JD_j\phi^J+D_i\chi^KD_j\chi^K\\&-\frac{1}{8}D_iD_j\big(\chi^K\big)^2+\frac{1}{2}\bar\psi^L\gamma_{(i}\overleftrightarrow{D}_{j)}\psi^L\\&-\delta_{ij}\bigg(\frac{1}{2}F^I_{kl}F^{Ikl}+\frac{1}{2}\big(D\phi^J\big)^2+\frac{1}{2}\big(D\chi^K\big)^2-\frac{1}{8}D^2\big(\chi^K\big)^2\\&+\lambda_{M_1M_2M_3M_4}\Phi^{M_1}\Phi^{M_2}\Phi^{M_3}\Phi^{M_4}+\mu^{\alpha\beta}_{ML_1L_2}\Phi^{M}\psi^{L_1}_{\alpha}\psi^{L_2}_{\beta}\bigg)\Big].\end{aligned} \tag{9.68}$$

9.4.2 Calculating the Holographic Power Spectra

To extract predictions, we need to compute the coefficients $A(\bar q)$ and $B(\bar q)$ appearing in the general decomposition (9.44) of the stress tensor 2-point function, analytically continue the results, and then insert them in the holographic formulae (9.66) for the power spectra. This task is made somewhat simpler by the generalised conformal structure and large-$\bar N$ counting, which together imply that the general form of the 2-point function at large $\bar N$ is

$$A(\bar q)=\bar q^3\bar N^2f_A\big(g^2_{\mathrm{eff}}\big),\qquad B(\bar q)=\bar q^3\bar N^2f_B\big(g^2_{\mathrm{eff}}\big), \tag{9.69}$$

where $f_A(g^2_{\mathrm{eff}})$ and $f_B(g^2_{\mathrm{eff}})$ are general functions[8] of the dimensionless effective 't Hooft coupling

$$g^2_{\mathrm{eff}}=g^2_{\mathrm{YM}}\bar N/\bar q.$$

Under the QFT analytic continuations (9.17),

$$\bar N^2\bar q^3\to -iN^2q^3,\qquad g^2_{\mathrm{eff}}\to g^2_{\mathrm{eff}},$$

[8] If instead we had imposed only the generalised conformal structure and not the large-$\bar N$ counting, then the r.h.s. of (9.69) would be modified as $\bar N^2f(g^2_{\mathrm{eff}})\to f(\bar N^2,g^2_{\mathrm{eff}})$, where $f(\bar N^2,g^2_{\mathrm{eff}})$ is a general function of two variables.

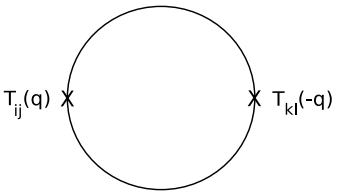

Fig. 9.2 1-loop contribution to the stress tensor 2-point function. We sum over the contributions from gauge fields, scalars and fermions, with each diagram yielding a contribution of order $\sim \bar{N}^2 \bar{q}^3$

hence $A(\bar{q})$ and $B(\bar{q})$ continue very simply in theories with generalised conformal invariance. (Recall here that the invariance of $g^2_{\rm eff}$ was our original reason for continuing $\bar{N} = -iN$ and not $\bar{N} = +iN$ in (9.17). The invariance of $g^2_{\rm eff}$ is required since $f_A(g^2_{\rm eff})$ and $f_B(g^2_{\rm eff})$ are in general non-analytic functions of $g^2_{\rm eff}$.) Inserting (9.69) into the holographic formulae (9.66) then, the cosmological power spectra are

$$\Delta^2_S(q) = \frac{1}{16\pi^2 N^2}\frac{1}{f_A(g^2_{\rm eff})}, \qquad \Delta^2_T(q) = \frac{2}{\pi^2 N^2}\frac{1}{f_B(g^2_{\rm eff})}. \tag{9.70}$$

In principle these formulae receive subleading $1/N^2$ corrections, however, as we shall see shortly, the observational data favour $N \sim 10^4$ rendering such terms negligible in practice. In the following, we now turn to evaluate the functions $f_A(g^2_{\rm eff})$ and $f_B(g^2_{\rm eff})$ in the perturbative limit where $g^2_{\rm eff}$ is small.

9.4.2.1 1-Loop Calculation

The leading contribution to the 2-point function of the stress tensor is at one loop (see Fig. 9.2). Since the stress tensor has dimension three, and the only dimensionful quantity that can appear to this order is $\bar{q}$ (1-loop amplitudes are independent of g^2_{YM}), it follows that

$$A(\bar{q}) = f^{(0)}_A \bar{N}^2 \bar{q}^3 + O\big(g^2_{\rm eff}\big), \qquad B(\bar{q}) = f^{(0)}_B \bar{N}^2 \bar{q}^3 + O\big(g^2_{\rm eff}\big), \tag{9.71}$$

i.e., $f_{A/B} = f^{(0)}_{A/B} + O(g^2_{\rm eff})$ where $f^{(0)}_{A/B}$ are numerical coefficients whose value depends only on the field content. Explicit calculation then reveals that

$$f^{(0)}_A = (\mathscr{N}_A + \mathscr{N}_\phi + \mathscr{N}_\chi + 2\mathscr{N}_\psi)/256, \qquad f^{(0)}_B = (\mathscr{N}_A + \mathscr{N}_\phi)/256. \tag{9.72}$$

Inserting this into our holographic formulae, we find

$$\Delta^2_S(q) = \frac{1}{16\pi^2 N^2 f^{(0)}_B} + O\big(g^2_{\rm eff}\big), \qquad \Delta^2_T(q) = \frac{2}{\pi^2 N^2 f^{(0)}_A} + O\big(g^2_{\rm eff}\big). \tag{9.73}$$

From an observational perspective, the cosmological power spectra are known to be well fitted by the empirical parametrisations

$$\Delta_S^2(q) = \Delta_S^2(q_*)\left(\frac{q}{q_*}\right)^{n_S(q)-1}, \qquad \Delta_T^2(q) = \Delta_T^2(q_*)\left(\frac{q}{q_*}\right)^{n_T(q)} \tag{9.74}$$

where $\Delta^2_{S/T}(q_*)$ is the scalar/tensor amplitude at some chosen pivot scale q_*, and $n_{S/T}(q)$ is the scalar/tensor spectral tilt. Comparing with (9.73), we see immediately that the power spectra are *scale-invariant* to leading order (i.e. $n_S = 1 + O(g^2_{\text{eff}})$, $n_T = O(g^2_{\text{eff}})$), regardless of the precise field content of the model. To estimate the value of N we may compare with the observed amplitude of the scalar power spectrum. From the WMAP data [25] we have $\Delta^2_S(q_*) \sim O(10^{-9})$, hence $N \sim O(10^4)$, justifying our use of the large N limit.

The observational data also serve to provide an upper bound on the ratio of tensor to scalar power spectra. From (9.73), we find

$$r = \Delta_T^2/\Delta_S^2 = 32 f_B^{(0)}/f_A^{(0)} + O\big(g^2_{\text{eff}}\big),$$

and hence an upper bound on r translates into a constraint on the field content of the dual QFT through (9.72). A smaller upper bound on r requires increasing the number of conformal scalars and massless fermions and/or decreasing the number of gauge fields and minimal scalars.

9.4.2.2 2-Loop Corrections

Corrections to the stress tensor 2-point function at 2-loop order give rise to small deviations from scale invariance. In the following we will focus on the case of the scalar power spectrum, since this is the more tightly constrained by observational data. (The behaviour of the tensor power spectrum is essentially identical, however, with only the values of the coefficients being different.) At 2-loop order then, either by inspection or from direct calculation of some of the contributing diagrams depicted in Fig. 9.3, the function $f_B(g^2_{\text{eff}})$ takes the form

$$f_B\big(g^2_{\text{eff}}\big) = f_B^{(0)}\big(1 - f_B^{(1)} g^2_{\text{eff}} \ln g^2_{\text{eff}} + f_B^{(2)} g^2_{\text{eff}} + O\big(g^4_{\text{eff}}\big)\big), \tag{9.75}$$

where $f_B^{(1)}$ and $f_B^{(2)}$ are numerical coefficients depending on the QFT field content, as well as the Yukawa and the quartic couplings.

As is well known, in perturbation theory super-renormalisable theories with massless fields display severe infrared divergences. Indeed, each of the 2-loop diagrams listed in Fig. 9.3 evaluates to an overall factor of $\bar{N}^3 g^2_{\text{YM}}$ multiplying an integral with superficial degree of (infrared) divergence two. Imposing an infrared

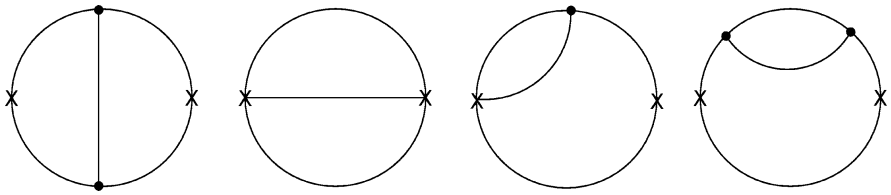

Fig. 9.3 Diagram topologies contributing at 2-loop order

cut-off, $\bar{q}_{\rm IR}$, one may evaluate the integrals to obtain $\sim\bar{q}^2\ln(\bar{q}/\bar{q}_{\rm IR})$. Altogether, one finds a 2-loop contribution to the stress tensor 2-point function of the order

$$\bar{N}^2\bar{q}^3 g_{\rm eff}^2\ln(\bar{q}/\bar{q}_{\rm IR}) = \bar{N}^2\bar{q}^3\big(-g_{\rm eff}^2\ln g_{\rm eff}^2 + g_{\rm eff}^2\ln\big(g_{\rm YM}^2\bar{N}/\bar{q}_{\rm IR}\big)\big). \tag{9.76}$$

Thus, $f_B^{(1)}$ is determined by the full 2-loop calculation but $f_B^{(2)}$ remains undetermined, since $\bar{q}_{\rm IR}$ is so far arbitrary. It was argued in [19], however, that this infrared divergence is an artefact of perturbation theory and that instead the theory develops a physical scale that acts as a cut-off. To compute this scale generally requires non-perturbative information. For a specific class of models, it was shown in [2] that a large-$\bar{N}$ resummation leads to a finite answer with $\bar{q}_{\rm IR}\sim g_{\rm YM}^2\bar{N}$. Similar behaviour is expected for the class of QFTs we consider here, but a precise determination of the infrared scale $\bar{q}_{\rm IR}$ (and hence $f_B^{(2)}$) is not yet to hand.

Instead, we will simply assume that all the cosmological scales relevant to the CMB lie far above the infrared scale $\bar{q}_{\rm IR}$, allowing the effects of the latter to be neglected. The validity of this assumption may then be cross-checked through comparison with the observational data. To this end, we rearrange (9.75) in the form

$$f\big(g_{\rm eff}^2\big) = f_B^{(0)}\big(1 + f_B^{(1)}g_{\rm eff}^2\ln\big(1/\big(f_B^{(3)}g_{\rm eff}^2\big)\big) + O\big(g_{\rm eff}^4\big)\big), \tag{9.77}$$

where $f_B^{(3)} = \exp(-f_B^{(2)}/f_B^{(1)})$. Thus, as long as we probe the theory at momentum scales far above $\bar{q}_{\rm IR}$, the specific value of $f_B^{(3)}$ should only provide a small correction since $|\ln g_{\rm eff}^2| \gg |\ln f_B^{(3)}|$. We will thus write $f_B^{(3)} = \beta|f_B^{(1)}|$ and take $\beta = 1$ in the following. (For the effects of allowing the parameter β to vary, see [14].)

To simplify our notation, we set

$$f_B^{(1)}g_{\rm YM}^2\bar{N} = g\bar{q}_*, \tag{9.78}$$

where $\bar{q}_*$ is the pivot scale. Substituting back into (9.70), we obtain the following 2-loop approximation to the power spectrum[9]

[9]Note that in previous treatments [33–35] we chose to Taylor expand the result (9.79); here, we retain the full form to provide better accuracy in the case that gq_*/q is not so small.

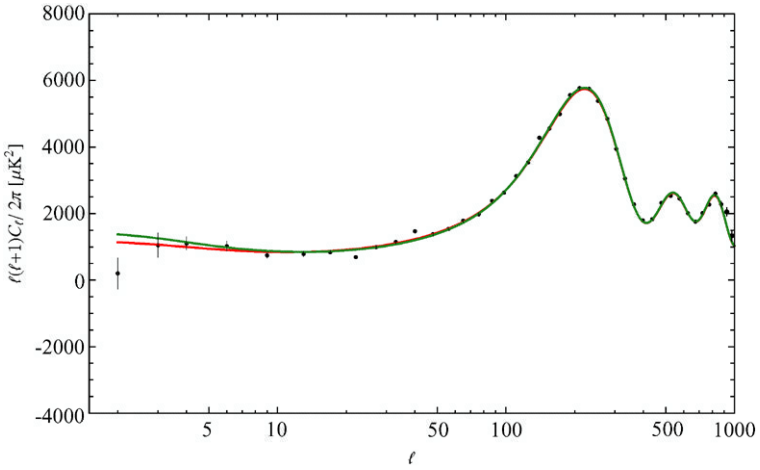

Fig. 9.4 Perturbative theoretical prediction for the power spectrum of the holographic model. The *lower curve* corresponds to $g > 0$ while the *upper* corresponds to $g < 0$. The perturbative calculation is reliable for $g_{\rm eff}^2 \sim gq_*/q \ll 1$, corresponding to large momenta $q/gq_* \gg 1$ far from the peak/trough feature at $\ln|q/gq_*| = 1$. At sufficiently high momenta, the power spectrum becomes nearly scale invariant, with $g > 0$ corresponding to a blue tilt and $g < 0$ to a red tilt

$$\Delta_S^2(q) = \Delta_S^2(q_*)\frac{1}{1 + (gq_*/q)\ln|q/gq_*|}, \tag{9.79}$$

where $\Delta_S^2(q_*) = 1/(4\pi^2 N^2 f_B^{(0)})$.

The power spectrum (9.79) is plotted in Fig. 9.4 for both positive and negative g. At sufficiently large momenta the spectrum rapidly becomes nearly scale invariant, with positive values of g resulting in a slight blue tilt and negative values of g yielding a slight red tilt. This behaviour reflects the fact that the dual QFT becomes asymptotically free at high momenta, with the free theory itself corresponding to an exact Harrison-Zel'dovich spectrum.

At lower momenta, the existence of the non-perturbative infrared scale $q_{\rm IR}$ becomes apparent, resulting in the peak/trough feature in the spectrum at $q = egq_*$. Note, however, that the perturbative calculation of $f_B(g_{\rm eff}^2)$ underpinning the power spectrum (9.79) breaks down when $g_{\rm eff}^2 \sim gq_*/q$ becomes of order unity (recalling that $f_B^{(1)}$ is a constant of order unity). This means that the perturbative result (9.79) becomes unreliable at low momenta close to the peak/trough feature in Fig. 9.4. Moreover, our approximation $\beta = 1$ is no longer justified in this regime and one should retain β as an independent parameter. Since the smallest momentum scale appearing in the CMB is of the order 10^{-4} Mpc^{-1}, if the power spectrum (9.79) is to reliably fit the entire range of CMB scales, then we conclude that the maximum value of g is restricted to be of the order $|g|_{\rm max} \sim 2 \times 10^{-3}$.

9.5 Confronting Observations

Having obtained the 2-loop approximation (9.79) to the holographic power spectrum, in this section we discuss its compatibility with the current observational data [14] (see also [13]). In addition to specifying the primordial power spectrum (9.79), we need to specify the matter content of the post-inflationary universe: for simplicity we will assume a six-parameter 'holographic-ΛCDM' model describing a flat universe with radiation, baryons, cold dark matter and a cosmological constant. Four of the six parameters thus describe the composition and expansion of the universe, namely the Hubble rate $H_0 = 100h$ km/s/Mpc, the physical baryon and dark matter densities $\Omega_b h^2$ and $\Omega_c h^2$, and the optical depth due to re-ionisation τ. (Given that we do not need spatial curvature to fit the data, the current dark energy contribution then follows from the requirement that the overall density of the universe is equal to the critical value.) The remaining two parameters are those featuring in the holographic power spectrum (9.79), namely the amplitude $\Delta_S^2(q_*)$ and the holographic coupling g. (The pivot scale is arbitrary and we will take it to be $\bar{q}_* = 0.05\ \mathrm{Mpc}^{-1}$.)

As a benchmark for the performance of the holographic model, we will also evaluate the performance the conventional power-law ΛCDM model. This latter model may be obtained by replacing the holographic power spectrum (9.79) with a spectrum of the power-law form (9.74), with the spectral index n_s assumed to be constant. (Such a power spectrum provides a good approximation to the predictions of simple conventional inflationary models, for which the running $\alpha_s = \mathrm{d}n_s/\mathrm{d}\ln q$ is of higher order in slow roll than the departure from scale invariance $n_s - 1$ [27].) Both ΛCDM and the holographic model thus have six parameters: in place of the holographic coupling g, ΛCDM has the spectral index n_s, with the other five parameters $\Omega_b h^2$, $\Omega_c h^2$, h, τ and $\Delta_s^2(q_*)$ being common to both models.

The best-fit values for the six parameters of the holographic-ΛCDM model are summarised[10] in Table 9.1, based on the analysis of [14]. Analogous results for power-law ΛCDM may be found in Table 9.2. The results are quoted both for the seven-year WMAP data [26], as well as for the combined data sets WMAP+BAO+H_0 and WMAP+CMB also introduced in [26]. (The former is a combination of WMAP7 with priors on the Hubble constant [41] and angular diameter distances [40], while the latter is a combination of WMAP7 with small-scale CMB experiments.)

Comparing Tables 9.1 and 9.2, we see that the estimated values of those parameters common to both models are essentially overlapping, with only $\Omega_b h^2$ differing by about one standard deviation. The best-fit value of the holographic coupling g is as expected small, indicating a nearly scale-invariant spectrum. The best-fit value of g is not so small, however, that we can be fully comfortable with our approximation

[10]Note we have exchanged the dimensionless Hubble parameter h for the parameter θ denoting the ratio between the sound horizon at the time of last scattering and the angular diameter distance of the surface of last scattering. Physically, this ratio fixes the position of the acoustic peaks and is tightly constrained by the data. Theoretically, θ is a function of $\Omega_b h^2$, $\Omega_c h^2$ and h, hence given $\Omega_b h^2$ and $\Omega_c h^2$, θ may be expressed in terms of h (for more details see, e.g., Sect. 7.2 of [51]).

Table 9.1 Parameters of holographic-ΛCDM and their uncertainties at the 68 % confidence level

	WMAP7	WMAP+BAO+H_0	WMAP+CMB
$\Omega_b h^2$	0.02310 ± 0.00045	0.02312 ± 0.00043	0.02326 ± 0.00045
$\Omega_c h^2$	0.1077 ± 0.0051	0.1120 ± 0.0036	0.1076 ± 0.0042
100θ	1.0407 ± 0.0026	1.0406 ± 0.0026	1.0423 ± 0.0022
τ	0.087 ± 0.015	0.084 ± 0.015	0.088 ± 0.016
Δ_S^2	$(2.146 \pm 0.088) \times 10^{-9}$	$(2.172 \pm 0.086) \times 10^{-9}$	$(2.151 \pm 0.084) \times 10^{-9}$
g	-0.00127 ± 0.00093	-0.00136 ± 0.00094	-0.00114 ± 0.00088

Table 9.2 Parameters of power-law ΛCDM and their uncertainties at the 68 % confidence level

	WMAP7	WMAP+BAO+H_0	WMAP+CMB
$\Omega_b h^2$	0.02252 ± 0.00056	0.02257 ± 0.00053	0.02265 ± 0.00051
$\Omega_c h^2$	0.1116 ± 0.0054	0.1127 ± 0.0035	0.1124 ± 0.0048
100θ	1.0394 ± 0.0027	1.0400 ± 0.0026	1.0411 ± 0.0022
τ	0.088 ± 0.014	0.088 ± 0.014	0.088 ± 0.014
$\Delta_S^2(q_*)$	$(2.183 \pm 0.073) \times 10^{-9}$	$(2.191 \pm 0.075) \times 10^{-9}$	$(2.190 \pm 0.068) \times 10^{-9}$
n_s	0.969 ± 0.014	0.970 ± 0.012	0.969 ± 0.013

Table 9.3 Best-fit log likelihood values $-\ln \mathscr{L}$ for both the holographic model and ΛCDM, as well as the difference $\Delta \ln \mathscr{L} = \ln \mathscr{L}_{\Lambda\text{CDM}} - \ln \mathscr{L}_{\text{hol}}$ between them. The errors on the best-fit log likelihoods are estimated to be around 0.1

	Holographic Model	ΛCDM	$\Delta \ln \mathscr{L}_{\text{best}}$
WMAP7	3735.5	3734.3	1.2
WMAP+BAO+H_0	3737.3	3735.7	1.6
WMAP+CMB	3815.0	3812.5	2.5

$|g|q_*/q \ll 1$ used to derive the holographic power spectrum. At the lower end of the range of momentum scales contributing to the CMB, $q \approx 10^{-4}$ Mpc^{-1}, we find $|g|q_*/q \approx 0.65$, indicating that the higher-order loop corrections and the effects of the infrared scale are potentially becoming important. Understanding the magnitude and significance of these effects is an important goal for future work.

The best-fit log likelihoods for both models are summarised in Table 9.3. The likelihood function $\mathscr{L}(\alpha_M) \equiv P(D|\alpha_M)$ encodes the probability of obtaining the data D, given the model M with some choice of parameters α_M. Thus, from Table 9.3, the probability of obtaining the observed WMAP7 data is approximately three times as likely given the power-law ΛCDM model with all parameters set to their best-fit values as for the holographic model, also with its parameters set to their best-fit values. Power-law ΛCDM is therefore slightly better at fitting the data, as illustrated in Fig. 9.5.

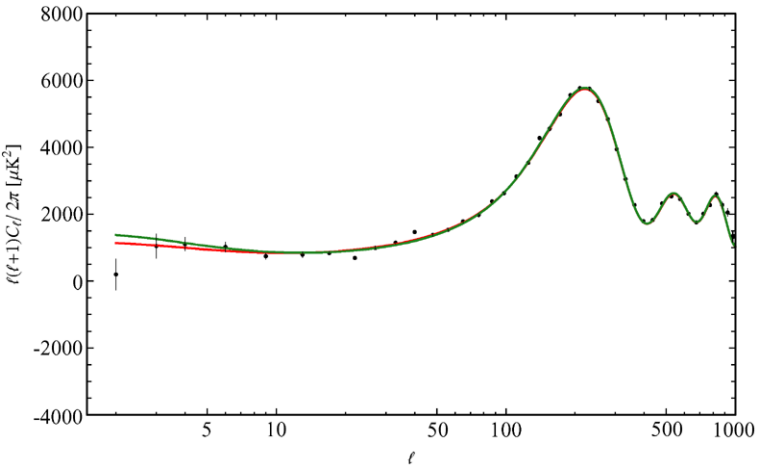

Fig. 9.5 Best-fit angular power spectra for power-law ΛCDM (*lower curve*, coloured red online) and holographic model (*upper curve*, coloured green online), versus the WMAP7 data

In performing a comparison of two models, however, the relevant quantity is *not* goodness of fit as measured by the best-fit log likelihood, but rather, the *Bayesian evidence* (see, e.g., [29] for an extended discussion). Given two models M_1 and M_2, we wish to evaluate which model is most probable given the data, i.e., the ratio

$$\frac{P(M_1|D)}{P(M_2|D)} = \frac{P(D|M_1)}{P(D|M_2)}\frac{P(M_1)}{P(M_2)},$$

where from Bayes' theorem

$$P(M_1|D) = \frac{P(D|M_1)P(M_1)}{P(D)}$$

and similarly for M_2. (The unconditional probability for the data $P(D)$ is a model-independent constant and so drops out of the ratio $P(M_1|D)/P(M_2|D)$.) Assuming that each model is a priori equally as likely so $P(M_1)/P(M_2)$ is unity, the relevant quantity to compute is then the *evidence ratio* E_1/E_2, where

$$E_1 \equiv P(D|M_1) = \int \mathrm{d}\alpha_{M_1}\, P(\alpha_{M_1})\mathscr{L}(\alpha_{M_1})$$

and similarly for M_2. The evidence thus naturally takes into account our uncertainty regarding the parameters of the model by integrating the likelihood over the entire parameter space, weighted by the prior probability $P(\alpha_M)$. (In contrast, the best-fit likelihood is simply the maximum value attained by the likelihood at any single point in this parameter space.)

To compute the evidence then, we need to assign prior probability distributions $P(\alpha_M)$ for the parameters of each model. If we assume flat priors, namely, a prior

probability that is constant over some defined region and zero outside, the evidence reduces to the integral

$$E = \frac{1}{\mathrm{Vol}_M} \int d\alpha_M \mathscr{L}(\alpha_M), \tag{9.80}$$

where Vol_M is the volume of the region in parameter space over which the prior probability distribution is non-zero. If the likelihood function is strongly peaked with support over only a relatively small region inside Vol_M, changing the prior region can strongly affect the computed evidence. Provided the changes to the overall volume of the parameter space do not add or exclude regions where $\mathscr{L}$ is large, the integral will be unaffected while Vol_M can change substantially, with the computed evidence being inversely proportion to Vol_M.

With the exception of n_s and g, both models have the same parameters. By using the same priors for the variables shared by the holographic and standard ΛCDM scenarios the ambiguity in the evidence associated with Vol_M is minimised. The situation with g and n_s is however more problematic. For the holographic model, we should restrict g to values where perturbative expansion used to derive (9.79) is valid. As we estimated at the end of Sect. 9.4.2.2, this corresponds to restricting $|g| < |g|_{\max} \approx 2 \times 10^{-3}$. (In fact the computed value of the evidence is only mildly dependent on the value of $|g|_{\max}$, as we will see in Figs. 9.6 and 9.7, see also [14].)

The choice prior for n_s is less straightforward since, unlike $|g|_{\max}$, the spectral index is a purely empirical parameter and we cannot restrict it by appealing to the internal consistency of some underlying theory. Moreover, our best information about n_s is derived from the WMAP data we are using to compute the evidence, and it would be inappropriately circular to set the prior on n_s directly from a parameter estimate derived from the WMAP data itself! To illustrate the consequences of this dilemma, we will consider two different choices of prior, $0.92 < n_s < 1.0$ and $0.9 < n_s < 1.1$. The first choice includes only the range over which the likelihood is appreciably different from zero, maximising the evidence for ΛCDM at the risk of being circular. The second choice is centered symmetrically on the scale-invariant Harrison-Zel'dovich spectrum, and hence does not provide any information about the sign of n_s. (In this sense the second choice is fairer, since we do not provide the holographic model with the sign of the tilt, corresponding to the sign of g, either.)

The result of the evidence calculation for the WMAP7 data set is presented in Fig. 9.6, and the results including the other data sets are given in Fig. 9.7. (Details of the numerical implementation of the computation and the choice of priors for the parameters common to both models may be found in [14].) Examining the plots, if we assume the narrow prior of $0.92 < n_2 < 1$, we find the difference in $-\ln E$ is of order 1.2 to 1.6, which corresponds to weak evidence in favour of ΛCDM. The difference in evidence is slightly more pronounced for the combined data sets WMAP7+BAO+H_0 and WMAP+CMB when compared to the pure WMAP7 data set. On the other hand, for the wider prior of $0.9 < n_s < 1.1$, the difference in evidence is less than unity, and as such is not considered statistically significant. Regardless of which prior is used, we do not find any strong evidence in favour of ΛCDM, where 'strong' evidence is generally taken to mean differences in $-\ln E$

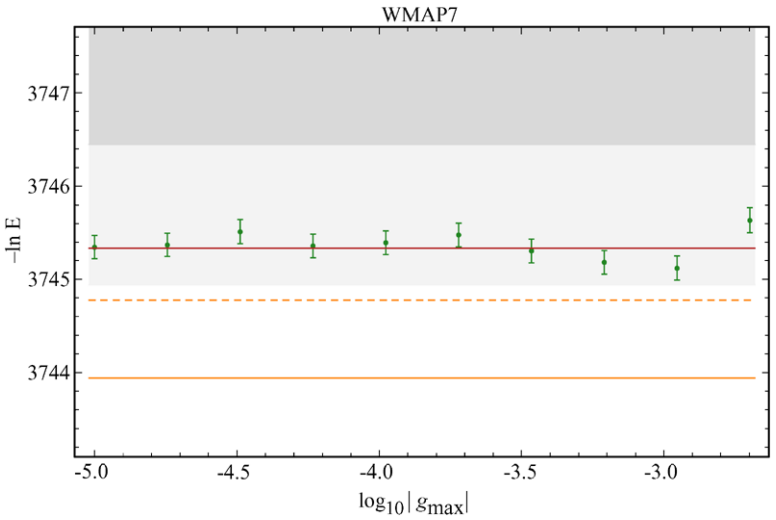

Fig. 9.6 The Bayesian evidence for the WMAP7 data set. The ΛCDM model with the narrow and broad priors corresponds to the *lowermost solid line* and the *middle dashed line* respectively (coloured orange online). The *uppermost solid line* (*red*) is the evidence for the pure Harrison-Zel'dovich spectrum with $n_s = 1$. The data points represent evidence computed for the holographic model, as a function of $|g|_{\max}$, as indicated on the horizontal axis. As a guide to the eye, the shading indicates differences in evidence $\Delta \ln E$ of 1, 2.5 and 5 relative to ΛCDM with the narrow prior (i.e., relative to the lowermost solid line)

of greater than 2.5. At this stage then, the only firm conclusion that can be drawn is that better data is required. Fortunately, with the imminent release of data from the Planck satellite we will not have long to wait.

An important clue to the theoretical issues at stake is provided by comparing the evidence for the holographic model with that of the exactly scale-invariant Harrison-Zel'dovich spectrum. From Figs. 9.6 and 9.7, we find that the computed evidence for both models is roughly identical. With hindsight, this is perhaps not too surprising since the holographic power spectrum coincides with the Harrison-Zel'dovich spectrum when the holographic coupling $g = 0$ (i.e., when the dual QFT is free). Moreover, to ensure the validity of the perturbative calculation underpinning the holographic power spectrum (9.79) across the entire range of CMB momentum scales, we restricted the maximum value of the holographic coupling to $|g| < |g|_{\max}$. In effect, this restriction limits the amount of scale-dependence that may be obtained from the holographic model, accounting for its similarity in performance to the Harrison-Zel'dovich spectrum.

A number of potential approaches to this problem present themselves: the most conservative would be to improve our determination of $g_{\max}$ by computing the unknown coefficient $f_B^{(1)}$ at 2-loop order (the result will in general depend on the Yukawa and quartic couplings, as well as the field content of the dual QFT). It may be that the simple order-of-magnitude estimate of $|g|_{\max}$ used here is too small, meaning that our perturbative calculation in fact allows more scale-dependence than

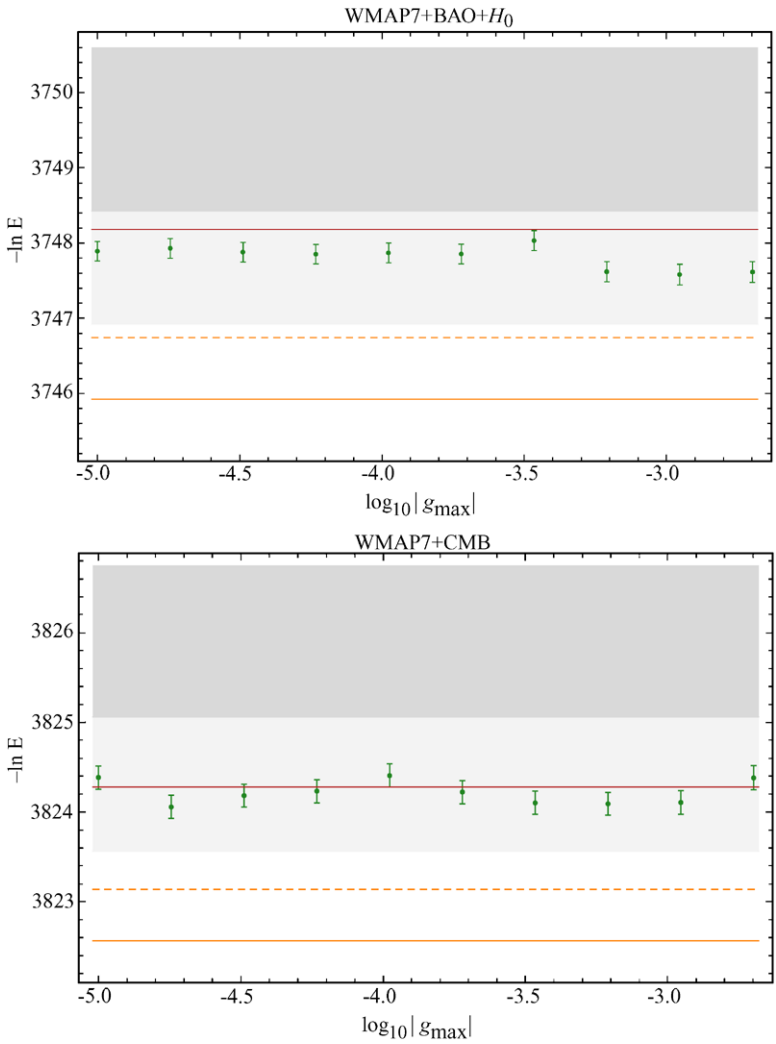

Fig. 9.7 The Bayesian evidence for the WMAP7+BAO+H_0 and WMAP7+CMB data sets, displayed using the same conventions as in Fig. 9.6

we have permitted here. An improved understanding of the infrared scale is also required to determine how far we may push our perturbative calculation of the power spectrum. A more radical approach would be to relax the assumption that the dual QFT should be perturbative over the entire range of CMB momentum scales, and instead permit g^2_{eff} to become large at the lower end of the CMB range. To pursue this connection, it would be interesting to see if $f_B(g^2_{\text{eff}})$, and hence the holographic power spectrum, could be computed numerically via lattice simulations.

9.6 Conclusion

In this article, we presented a holographic framework for inflationary cosmology, based on standard holography in combination with the domain-wall/cosmology correspondence. Cosmological observables are related by this framework to correlation functions of a dual three-dimensional QFT. The correlation functions of this dual QFT may be obtained by a straightforward analytic continuation of the correlators of the regular QFT dual to the corresponding domain-wall spacetime, at least within the context of large-N perturbation theory. Analysing the behaviour of linearised fluctuations, we obtained precise holographic formulae relating the scalar and tensor cosmological power spectra to the 2-point function of the stress tensor of the dual QFT.

When the dual QFT is strongly coupled, the gravitational description is weakly coupled and we recover the predictions of conventional inflationary scenarios, albeit from a holographic perspective. When the dual QFT is weakly coupled, however, we obtain a scenario in which the gravitational description is strongly coupled at early times, describing an early universe which is in a non-geometric phase. In general, there are two classes of dual QFT for which the holographic description is comparatively well understood. The first class comprises deformations of conformal field theories, and corresponds to universes which are asymptotically de Sitter towards the end of the inflationary epoch. The properties and phenomenology of these models is relatively unexplored and is a major direction for future research. The second class, on which we focused here, describe QFTs with generalised conformal symmetry and correspond to universes whose geometry is asymptotically power-law towards the end of the inflationary era. Dual QFTs of this form are super-renormalisable and are moreover free from infrared divergences, offering in principle a complete description of the corresponding cosmological evolution. For this class of models, we saw how to compute the scalar and tensor cosmological power spectra explicitly up to 2-loops in perturbation theory.

The overall amplitude of the power spectrum is proportional to $1/N^2$, implying that $N \sim O(10^4)$ in accordance with the large-N limit. At leading 1-loop order, the power spectrum is moreover scale-invariant on simple dimensional grounds, with small deviations from scale invariance arising only from corrections at 2-loop order in perturbation theory. The validity of perturbation theory (or equivalently, the assumed strong coupling of the gravitational description at early times) is therefore directly linked to the near scale-invariance of the observed power spectrum. A custom fit of the predicted 2-loop holographic power spectrum to WMAP7 and other astrophysical data sets confirms that these predictions are indeed fully compatible with current observational data. Nevertheless, there are strong prospects for observationally distinguishing the holographic-ΛCDM model from conventional power-law ΛCDM following the release of data from the Planck satellite and other forthcoming observational probes. In particular, the holographic power spectrum rapidly becomes scale invariant at high momenta, essentially as a consequence of asymptotic freedom in the dual QFT. This generates a relatively strong running of the power spectrum, in which successive logarithmic derivatives $\mathrm{d}^k n_s(q)/\mathrm{d}\ln q^k$ are of

comparable order, in sharp contrast to conventional inflationary models for which successive logarithmic derivatives are of higher order in slow roll.

Some theoretical issues concerning the holographic power spectrum nonetheless remain. One of the most pressing is the need to determine more accurately the range of validity of the 2-loop approximation to the power spectrum, motivating a full 2-loop calculation as well as a detailed investigation of the effects of the non-perturbative infrared scale. Needless to say, should the future observational data definitively rule out a primordial power spectrum of the form we have considered here, only the specific class of dual QFTs possessing generalised conformal symmetry would be ruled out, rather than the notion of holography for cosmology per se. In this eventuality, one would then be able to focus exclusively on QFTs describing deformations of conformal field theories.

Another important issue for models assuming a strongly coupled gravitational description at early times is the exact nature of the post-inflationary transition to a conventional weakly coupled hot big bang phase. It would be very interesting to develop a detailed theory for this transition period, the analogue of the reheating period in conventional scenarios. In order to exit the holographic period we would need to modify the UV structure of the dual QFT (since the UV of the QFT corresponds to late times), which may be achieved by adding irrelevant operators to the QFT. At momenta far below the momentum scale q_{UV} set by the lowest dimension irrelevant operator, the computation of the 2-point function (and therefore of the power spectrum) is however well approximated by the computation we performed here. Thus, as long as q_{UV} is much larger that the largest momentum scale seen by CMB (i.e., $q_{UV} \gg 10^{-1}$ Mpc^{-1}), the error incurred by omitting this exit period is very small. In principle, though, one could compute corrections to the holographic formulae due to such irrelevant operators and extract from the data the best-fit value for q_{UV}. We leave such a study for future work, but note that the ability to fit the data well without these corrections suggests they are indeed small.

A final topic we have not discussed here is the predictions of holographic models for primordial non-Gaussianity. Up to the level of the 3-point function, these predictions have been calculated in great detail in [7, 36, 37]. As one might expect, cosmological 3-point functions are related via holographic formulae to 3-point functions of the stress tensor of the dual QFT. The analysis is of essentially the same character as that studied here for the holographic power spectrum, though the necessity of working at quadratic order in perturbation theory leads to a somewhat greater technical complexity. A consideration of special importance is the appearance of 'semi-local' contact terms in the holographic formulae: these terms contribute when two of the three points in a 3-point function are coincident. From a purely QFT perspective one might be tempted to discard terms of this form, however when inserted into the relevant holographic formulae they contribute to 'local'-type cosmological non-Gaussianity and so must be retained. Intriguingly, for model QFTs of the type considered here, the cosmological scalar bispectrum is predicted [37] to be of *exactly* the equilateral template (to our knowledge, the only model known to do so), with the nonlinearity parameter $f_{\rm NL} = 5/36$. Remarkably, this value for $f_{\rm NL}$ is a concrete prediction fully independent of the field content of the dual QFT. The analogous predictions for 3-point functions involving tensors were determined in [7]. In

particular, for the case of three gravitons, one may recover the *exact* 3-point function of conventional slow-roll inflation, extending the result recently reported in [32].

To conclude, let us remind ourselves of some of the many pressing questions that remain. Can we use the holographic description to enhance our understanding of inflationary fine tunings? Is there a holographic description for the late-time de Sitter epoch we find ourselves entering, and if so, what are the consequences? Can we understand the entropy of de Sitter space holographically?

Acknowledgements I am grateful to the organisers of the Sixth Aegean Summer School for a stimulating conference and an exciting opportunity to present this work, as well as to my collaborators Adam Bzowski, Richard Easther, Raphael Flauger and Kostas Skenderis with whom this work was developed. This research was funded through a VENI grant from NWO, the Netherlands Organisation for Scientific Research.

References

1. D. Anninos, T. Hartman, A. Strominger, Higher spin realization of the DS/CFT correspondence (2011). arXiv:1108.5735
2. T. Appelquist, R.D. Pisarski, High-temperature Yang-Mills theories and three-dimensional quantum chromodynamics. Phys. Rev. D **23**, 2305 (1981). doi:10.1103/PhysRevD.23.2305
3. M. Bianchi, D.Z. Freedman, K. Skenderis, How to go with an RG flow. J. High Energy Phys. **0108**, 041 (2001)
4. M. Bianchi, D.Z. Freedman, K. Skenderis, Holographic renormalization. Nucl. Phys. B **631**, 159–194 (2002)
5. H.J. Boonstra, K. Skenderis, P.K. Townsend, The domain wall/QFT correspondence. J. High Energy Phys. **01**, 003 (1999)
6. R.H. Brandenberger, Inflationary cosmology: progress and problems (1999). hep-ph/9910410
7. A. Bzowski, P. McFadden, K. Skenderis, Holographic predictions for cosmological 3-point functions (2011). arXiv:1112.1967
8. P. Creminelli, A. Nicolis, M. Zaldarriaga, Perturbations in bouncing cosmologies: dynamical attractor versus scale invariance. Phys. Rev. D **71**, 063505 (2005). doi:10.1103/PhysRevD.71.063505
9. M. Cvetic, H.H. Soleng, Naked singularities in dilatonic domain wall space times. Phys. Rev. D **51**, 5768–5784 (1995). doi:10.1103/PhysRevD.51.5768
10. J. de Boer, E.P. Verlinde, H.L. Verlinde, On the holographic renormalization group. J. High Energy Phys. **08**, 003 (2000)
11. S. de Haro, S.N. Solodukhin, K. Skenderis, Holographic reconstruction of spacetime and renormalization in the AdS/CFT correspondence. Commun. Math. Phys. **217**, 595–622 (2001). doi:10.1007/s002200100381
12. O. DeWolfe, D.Z. Freedman, S.S. Gubser, A. Karch, Modeling the fifth dimension with scalars and gravity. Phys. Rev. D **62**, 046008 (2000). doi:10.1103/PhysRevD.62.046008
13. M. Dias, Cosmology at the boundary of de Sitter using the dS/QFT correspondence. Phys. Rev. D **84**, 023512 (2011). doi:10.1103/PhysRevD.84.023512
14. R. Easther, R. Flauger, P. McFadden, K. Skenderis, Constraining holographic inflation with WMAP. JCAP **1109**(030) (2011). doi:10.1088/1475-7516/2011/09/030
15. D.Z. Freedman, C. Nunez, M. Schnabl, K. Skenderis, Fake supergravity and domain wall stability. Phys. Rev. D **69**, 104027 (2004). doi:10.1103/PhysRevD.69.104027
16. S. Gubser, I.R. Klebanov, A.M. Polyakov, Gauge theory correlators from noncritical string theory. Phys. Lett. B **428**, 105–114 (1998). doi:10.1016/S0370-2693(98)00377-3

17. M. Henningson, K. Skenderis, The holographic Weyl anomaly. J. High Energy Phys. **9807**, 023 (1998)
18. N. Itzhaki, J.M. Maldacena, J. Sonnenschein, S. Yankielowicz, Supergravity and the large N limit of theories with sixteen supercharges. Phys. Rev. D **58**, 046004 (1998). doi:10.1103/PhysRevD.58.046004
19. R. Jackiw, S. Templeton, How superrenormalizable interactions cure their infrared divergences. Phys. Rev. D **23**, 2291 (1981). doi:10.1103/PhysRevD.23.2291
20. A. Jevicki, T. Yoneya, Space-time uncertainty principle and conformal symmetry in D-particle dynamics. Nucl. Phys. B **535**, 335–348 (1998). doi:10.1016/S0550-3213(98)00578-1
21. A. Jevicki, Y. Kazama, T. Yoneya, Quantum metamorphosis of conformal transformation in D3-brane Yang-Mills theory. Phys. Rev. Lett. **81**, 5072–5075 (1998). doi:10.1103/PhysRevLett.81.5072
22. A. Jevicki, Y. Kazama, T. Yoneya, Generalized conformal symmetry in D-brane matrix models. Phys. Rev. D **59**, 066001 (1999). doi:10.1103/PhysRevD.59.066001
23. I. Kanitscheider, K. Skenderis, Universal hydrodynamics of non-conformal branes. J. High Energy Phys. **04**, 062 (2009). doi:10.1088/1126-6708/2009/04/062
24. I. Kanitscheider, K. Skenderis, M. Taylor, Precision holography for non-conformal branes. J. High Energy Phys. **09**, 094 (2008). doi:10.1088/1126-6708/2008/09/094
25. E. Komatsu et al., Five-year Wilkinson Microwave Anisotropy Probe (WMAP) observations: cosmological interpretation. Astrophys. J. Suppl. **180**, 330–376 (2009). doi:10.1088/0067-0049/180/2/330
26. E. Komatsu et al., Seven-year Wilkinson Microwave Anisotropy Probe (WMAP) observations: cosmological interpretation. Astrophys. J. Suppl. **192**, 18 (2011). doi:10.1088/0067-0049/192/2/18
27. A. Kosowsky, M.S. Turner, CBR anisotropy and the running of the scalar spectral index. Phys. Rev. D **52**, 1739–1743 (1995). doi:10.1103/PhysRevD.52.R1739
28. D. Langlois, Lectures on inflation and cosmological perturbations. Lect. Notes Phys. **800**, 1–57 (2010). doi:10.1007/978-3-642-10598-21
29. D. MacKay, *Information Theory, Inference, and Learning Algorithms* (Cambridge University Press, Cambridge, 2003). Available online at http://www.inference.phy.cam.ac.uk/mackay/itila/book.html
30. J.M. Maldacena, The large N limit of superconformal field theories and supergravity. Adv. Theor. Math. Phys. **2**, 231–252 (1998). doi:10.1023/A:1026654312961
31. J.M. Maldacena, Non-Gaussian features of primordial fluctuations in single field inflationary models. J. High Energy Phys. **05**, 013 (2003)
32. J.M. Maldacena, G.L. Pimentel, On graviton non-Gaussianities during inflation. J. High Energy Phys. **1109**, 045 (2011). doi:10.1007/JHEP09(2011)045
33. P. McFadden, K. Skenderis, Holography for cosmology. Phys. Rev. D **81**, 021301 (2010). doi:10.1103/PhysRevD.81.021301
34. P. McFadden, K. Skenderis, Observational signatures of holographic models of inflation, in *Proceedings of 12th Marcel Grossmann Meeting*, (2010) arXiv:1010.0244
35. P. McFadden, K. Skenderis, The holographic Universe. J. Phys. Conf. Ser. **222**, 012007 (2010)
36. P. McFadden, K. Skenderis, Cosmological 3-point correlators from holography. J. Cosmol. Astropart. Phys. **1106**, 030 (2011). doi:10.1088/1475-7516/2011/06/030
37. P. McFadden, K. Skenderis, Holographic non-Gaussianity. J. Cosmol. Astropart. Phys. **1105**, 013 (2011). doi:10.1088/1475-7516/2011/05/013
38. I. Papadimitriou, K. Skenderis, AdS/CFT correspondence and geometry, in *Proceedings of the Strasburg Meeting on AdS/CFT* (2004). hep-th/0404176
39. I. Papadimitriou, K. Skenderis, Correlation functions in holographic RG flows. J. High Energy Phys. **10**, 075 (2004). doi:10.1088/1126-6708/2004/10/075
40. B.A. Reid et al., Baryon acoustic oscillations in the Sloan digital sky survey data release 7 galaxy sample. Mon. Not. R. Astron. Soc. **401**, 2148–2168 (2010). doi:10.1111/j.1365-2966.2009.15812.x

41. A.G. Riess, L. Macri, S. Casertano, M. Sosey, H. Lampeitl et al., A redetermination of the Hubble constant with the Hubble space telescope from a differential distance ladder. Astrophys. J. **699**, 539–563 (2009). doi:10.1088/0004-637X/699/1/539
42. D.S. Salopek, J.R. Bond, Nonlinear evolution of long wavelength metric fluctuations in inflationary models. Phys. Rev. D **42**, 3936–3962 (1990). doi:10.1103/PhysRevD.42.3936
43. K. Skenderis, Lecture notes on holographic renormalization. Class. Quantum Gravity **19**, 5849–5876 (2002). doi:10.1088/0264-9381/19/22/306
44. K. Skenderis, P.K. Townsend, Gravitational stability and renormalization-group flow. Phys. Lett. B **468**, 46–51 (1999). doi:10.1016/S0370-2693(99)01212-5
45. K. Skenderis, P.K. Townsend, Hidden supersymmetry of domain walls and cosmologies. Phys. Rev. Lett. **96**, 191301 (2006). doi:10.1103/PhysRevLett.96.191301
46. K. Skenderis, B.C. van Rees, Real-time gauge/gravity duality. Phys. Rev. Lett. **101**, 081,601 (2008). doi:10.1103/PhysRevLett.101.081601
47. L. Susskind, The World as a hologram. J. Math. Phys. **36**, 6377–6396 (1995). doi:10.1063/1.531249
48. G. 't Hooft, A planar diagram theory for strong interactions. Nucl. Phys. B **72**, 461 (1974). doi:10.1016/0550-3213(74)90154-0
49. G. 't Hooft, Dimensional reduction in quantum gravity (1993). gr-qc/9310026
50. N. Turok, A critical review of inflation. Class. Quantum Gravity **19**, 3449–3467 (2002). doi:10.1088/0264-9381/19/13/305
51. S. Weinberg, *Cosmology* (Oxford University Press, Oxford, 2008)
52. T. Wiseman, B. Withers, Holographic renormalization for coincident Dp-branes. J. High Energy Phys. **10**, 037 (2008). doi:10.1088/1126-6708/2008/10/037
53. E. Witten, Anti-de Sitter space and holography. Adv. Theor. Math. Phys. **2**, 253–291 (1998)